TITLE PAGE

Advantages of a city-scale emission inventory for urban air quality research and policy: the case of Nanjing, a typical industrial city in the Yangtze River Delta, China

Yu Zhao[1,2,*,#], Liping Qiu[1,#], Runying Xu[1], Fangjian Xie[3], Qiang Zhang[4], Yiyong Yu[5], Chris P. Nielsen[6], Haixu Qin[3], Haikun Wang[1], Xiucai Wu[1], Wenqing Li[3], Jie Zhang[2,7]

1. State Key Laboratory of Pollution Control & Resource Reuse and School of the Environment, Nanjing University, 163 Xianlin Ave., Nanjing, Jiangsu 210023, China

2. Jiangsu Collaborative Innovation Center of Atmospheric Environment and Equipment Technology (CICAEET), Nanjing University of Information Science & Technology, Jiangsu 210044, China

3. Nanjing Academy of Environmental Protection Science, 175 Huju Rd., Nanjing, Jiangsu 210013, China

4. Ministry of Education Key Laboratory for Earth System Modeling, Center for Earth System Science, Tsinghua University, Beijing 100084, China

5. Nanjing Environmental Monitoring Central Station, 175 Huju Rd., Nanjing, Jiangsu 210013, China

6. Harvard China Project, School of Engineering and Applied Sciences, Harvard University, 29 Oxford St, Cambridge, MA 02138, USA

7. Jiangsu Provincial Academy of Environmental Science, 176 North Jiangdong Rd., Nanjing, Jiangsu 210036, China

# Joint first authors. Y. Z and L. Q contributed equally to this work.

* Corresponding author: Phone: 86-25-89680650; email: yuzhao@nju.edu.cn

ABSTRACT

With most eastern Chinese cities facing major air quality challenges, there is a strong need for city-scale emission inventories for use in both chemical transport modeling and the development of pollution control policies. In this paper, a high-resolution emission inventory (with a horizontal resolution at 3×3 km) of air pollutants and CO_2 for Nanjing, a typical large city in the Yangtze River Delta, is developed incorporating the best available information on local sources. Emission factors and activity data at the unit or facility level are collected and compiled using a thorough onsite survey of major sources. Over 900 individual plants, which account for 97% of the city's total coal consumption, are identified as point sources, and all of the emission-related parameters including combustion technology, fuel quality, and removal efficiency of air pollution control devices (APCD) are analyzed. New data-collection approaches including continuous emission monitoring systems and real-time monitoring of traffic flows are employed to improve spatiotemporal distribution of emissions. Despite fast growth of energy consumption between 2010 and 2012, relatively small inter-annual changes in emissions are found for most air pollutants during this period, attributed mainly to benefits of growing APCD deployment and the comparatively strong and improving regulatory oversight of the large point sources that dominate the levels and spatial distributions of Nanjing emissions overall. The improvement of this city-level emission inventory is indicated by comparisons with observations and other inventories at larger spatial scale. Relatively good spatial correlations are found for SO_2, NO_X, and CO between the city-scale emission estimates and concentrations at 9 state-opertated monitoring sites (R=0.58, 0.46, and 0.61, respectively). The emission ratios of specific pollutants including BC to CO, OC to EC, and CO_2 to CO compare well to top-down constraints from ground observations. The inter-annual variability and spatial distribution of NO_X emissions are consistent with NO_2 vertical column density measured by the Ozone

Monitoring Instrument (OMI). In particular, the Nanjing city-scale emission inventory correlates better with satellite observations than the downscaled Multi-resolution Emission Inventory for China (MEIC) does when emissions from power plants are excluded. This indicates improvement in emission estimation for sectors other than power generation, notably industry and transportation. High-resolution emission inventory may also provide a basis to consider the quality of instrumental observations. To further improve emission estimation and evaluation, more measurements of both emission factors and ambient levels of given pollutants are suggested; the uncertainties of emission inventories at city scale should also be fully quantified and compared with those at national scale.

1 INTRODUCTION

Emission inventories are crucial for atmospheric science research, particularly chemical transport modeling (CTM), and for air quality policymaking that seeks to identify and control pollution sources. Given China's important role in the origins and transport of air pollutants in East Asia and beyond, a number of emission inventories at national scale have been established in recent years. These include the Transport and Chemical Evolution over the Pacific Mission (TRACE-P, Streets et al., 2003), the Intercontinental Chemical Transport Experiment-Phase B (INTEX-B, Zhang et al., 2009), the Regional Emission inventory in ASia (REAS, Ohara et al., 2007; Kurokawa et al., 2013), and the Multi-resolution Emission Inventory for China (MEIC, http://www.meicmodel.org/). Based on "bottom-up" principles and frameworks similar to those described in Streets et al. (2003), more detailed source categories and expanded domestic information on emission factors and activity levels have been integrated into most recent work, yielding improved inter-annual trends in national estimates of anthropogenic air pollutant emissions (e.g., MEIC; Zhao et al., 2012a; 2012b; 2013). Aside from the national-level work, regional emission

55 inventories have also been established with improved understanding of local
56 conditions for key areas with high densities of population, industry, and energy
57 consumption, e.g., the Jing-Jin-Ji region including Beijing and Tianjin (JJJ; S. Wang
58 et al., 2010), the Yangtze River Delta (YRD; Fu et al., 2013; Huang et al., 2011), and
59 the Pearl River Delta (PRD; Zheng et al., 2009).

60 There is still need for improvement of bottom-up emission inventories, however,
61 particularly at smaller spatial scales. First, data for activity levels and emission factors
62 used in current Chinese inventories come mostly from coarse statistics or surveys at
63 the provincial level, except for select sectors (e.g., power generation, Zhao et al.,
64 2008). Underlying information that is crucial to emission levels (e.g., combustion or
65 manufacturing technologies, fuel qualities, and penetrations and removal efficiencies
66 of various emission control devices) has often been overlooked or assumed to be
67 uniform, inevitably reducing the accuracy and reliability of emission estimates.
68 Without sufficient source-specific information, in particular, it is hard to identify and
69 characterize "super-emitting" sources, which can strongly affect aggregate emission
70 estimates. Second, the spatial and temporal distributions of emissions are often not
71 well characterized. Emissions from most sectors are spatially allocated according to
72 proxies, e.g., population or economic densities. However, the distribution of large
73 sources in China is changing quickly because much industrial production is being
74 relocated out of urban cores, and the correlations between emissions and the usual
75 proxies like population density are getting weaker, particularly in developed cities
76 (Zhang et al., 2012a; Zhao et al., 2013). This introduces error into the spatial
77 allocations. The time distribution of emissions is commonly based on expert judgment,
78 with little reliance on real-time data sources, e.g., continuous emission monitoring
79 systems (CEMS). Finally, some sources that may play important roles in local
80 emissions are often missed in regional emission inventories, e.g., fugitive dust from
81 construction and road transportation, and volatile organic compounds (VOC) from gas
82 stations, mainly due to data limits on such sources. Such limitations weaken capacities

to research atmospheric chemistry using inventories as inputs to CTMs, and also undermine the efficacy of pollution control decision-making.

Several studies have illustrated the benefits of city-scale emission inventories that integrate more detailed local information. Timmermans et al. (2013), for example, concluded that the results of NO_2 and PM_{10} simulations were more consistent with observations for Paris when a local emission inventory was used. In the U.S., model simulations of NO_2 columns based on actual hourly NO_X emissions from CEMS agreed better with satellite observations than those based on default emission inputs from the U. S. Environmental Protection Agency (USEPA; Kim et al., 2009). In China, vehicle emission inventories resolved at the county level, rather than provincial level, were shown to better support air quality simulations for small regions (Zheng et al., 2014).

China is experiencing frequent severe haze episodes (Zhang et al., 2012b; Wang et al., 2013; Wang et al., 2014; R. Huang et al., 2014). Cities are being required to expand efforts at air pollution control, and use of CTMs for air quality assessment and policy making is becoming more routine. Due in part to weak emission inputs, however, atmospheric simulations for cities are often disappointingly inaccurate (personal communication with Zifa Wang from Institute of Atmospheric Physics, Chinese Academy of Science, 2014). Without integrating more detailed local information, some cities simply downscale a national emission inventory into high-resolution emission inputs for a CTM or develop local inventories based on the same source data and methods used for national ones. Despite improvements from some information (e.g., the precise location of large point sources), the quality and reliability of those inventories have not been well evaluated using, for example, integrated observational data as top-down constraints. Thus the emission estimates introduce large uncertainties into the city-scale air quality simulations.

It should be noted that such improvements in emission inventories for a few megacities, including Beijing and Shanghai, have been driven by air quality planning

for major events like the 2008 Summer Olympic Games and 2010 World Expo. During recent years, however, satellite observations have detected that the most significant growth in air pollution (indicated for example by vertical column densities of tropospheric NO_2) across the country is occurring not within such megacities but in the less-developed regions around them, due to faster growth in the economies and emission sources in those areas (Zhang et al., 2012a). This finding highlights the importance of developing and assessing air pollutant emission inventories for regions other than China's much-studied megacities.

We select Nanjing, a typical large city in the YRD, to establish and evaluate a high-resolution emission inventory at city scale. As shown in Figure S1(a) in the supplement, Nanjing is the capital city of Jiangsu Province and the second largest city in central east China following Shanghai, with a total area of 6587 km^2 and population of 8 million in 2012 (NJNBS, 2013). Intensively industrial, Nanjing consumes much more coal than many other Chinese cities with economies of similar size (e.g., Hangzhou, Qingdao, and Shenyang), and in 2012 suffered the highest number of days of haze (226) of all of China's provincial capital cities (data provided by the Nanjing Meteorological Bureau). The share of coal use in primary energy reached 89% in 2012 (Environmental Statistics, an internal database of the Nanjing Environmental Protection Bureau, NJEPB; NJNBS, 2013), much higher than the national level of 71% (NBSC, 2013). Large coal consumption and industrial and chemical production have resulted in high emissions of anthropogenic atmospheric pollutants. As the host city of the 2nd Asian Youth Games (AYG) in August 2013, Nanjing undertook various measures to control emissions in industry but allowed construction activities at thousands of sites, leading to large changes in the levels and the temporal and spatial distributions of emissions. Such changes are captured by a comprehensive city-scale emission inventory.

2 DATA AND METHODS

2.1 The basic methodology

The annual emissions in Nanjing from 2010 to 2012 are estimated with a bottom-up approach for 10 atmospheric pollutants (SO_2, NO_X, total suspended particulates (TSP), PM_{10}, $PM_{2.5}$, black carbon (BC) or elemental carbon (EC), organic carbon (OC), CO, VOCs, and NH_3) and the greenhouse gas CO_2. At the largest scale, sources fall into six main categories: coal-fired power plants (CPP), industry (IND), transportation (TRA, including on-road and non-road subcategories), the residential & commercial sector (RES, including fossil fuel, biofuel, and biomass open burning subcategories, along with gas stations for VOC estimation only), agriculture (AGR, including livestock farming and fertilizer use for NH_3 estimation only), and fugitive dust (FUD, including that from construction sites and roads). IND is further divided into cement plants (CEM), iron & steel plants (ISP), refineries and chemical plants (RCP), solvent use (SOL; although some solvent is not used in industry, we include it in this category for classification simplicity) and other industry plants (OIN).

To improve the accuracy and reliability of the city-level emission inventory, new data are collected from various sources and modified methods are applied compared to previous studies, as briefly summarized below.

With sufficient information related to emission estimation now available, more sources can be characterized as point sources in the current inventory. These include power plants (total number in 2012, similarly for subsequent categories: 18), cement plants (23), iron & steel plants (2), chemical plants (173), non-ferrous metal smelters (14), lime plants (9), brick plants (31), factories representing a portion of other industrial sectors (434), and gas-fueling stations (269). The locations of point sources by category are shown in Figure S1 (b) and (c) in the supplement. The annual emissions of point sources are calculated with Equation (1):

$$E_i = \sum_{j,m} A_{i,j,m} \times EF_{i,j,m} \times \left(1 - \eta_{i,j,m}\right) \quad (1)$$

where i, j and m represent the species, individual plant, and fuel/technology type, respectively; A is the activity level data; EF is the uncontrolled emission factor; and η is removal efficiency of air pollutant control device (APCD).

For all the point sources, information from the Environmental Statistics database and Pollution Source Census (internal data of NJEPB) is collected and compiled to obtain the activity levels (energy consumption or industrial production) and parameters related to emission factors, plant by plant. Moreover, we conduct onsite surveys individually for all of the CPP, CEM, ISP and RCP sources (labeled "key sources" in this paper), to get further information that is crucial for emission estimation but not covered by the official census or statistics (see details in Section 2.2). In 2012, all of the point sources and all of the key sources in Nanjing accounted for 97% and 96% of the city's total coal consumption, respectively, reflecting the highly centralized energy use of Nanjing. The annual activity levels for the key sources for 2010-2012 are summarized in Table S1 in the supplement.

Besides annual levels, monthly energy consumption, industrial production, and flue-gas concentrations from CEMS are obtained whenever possible through our plant-by-plant onsite investigations. The monthly distribution of emissions from key sources is then revised based on these data.

Emissions from on-road transportation are calculated using COPERT 4 (version 9.0) (EEA, 2012). The parameters required by the model, including vehicle population by type, fleet composition by control stage (China I-IV, equivalent to Euro I-IV), and annual average kilometers traveled (VKT), are taken from investigations by NJEPB. The detailed information for 2012 is summarized in Tables S2 and S3 in the supplement. The traffic flows in the city are compiled from the observations of the Intelligent Traffic Violation Monitoring System (internal data of NJEPB). In the system, cameras are used to continuously record the real-time traffic flows for most

arterial roads and highways, and part of residential roads in the city. The system does not cover all the roads (particularly for residential roads), and the traffic flows in those roads were simulated from the real-time monitoring data for similar roads that are covered by the system. Combining the information of traffic flows and the road net, the spatial and diurnal distributions of emissions from CORPERT can be derived. It should be noted, however, uncertainty exists in the allocation of vehicle emissions, particularly for areas with fewer cameras installed.

For area sources including other small industry, solvent use, residential combustion, agricultural activity, and non-road transportation, emissions are estimated following previous work (Zhao et al., 2012a; 2012b; 2013), with up-to-date emission factors from domestic measurements and city-scale activity levels. The energy consumption data are taken from the Environmental Statistics (internal data of NJEPB) and the agricultural and industrial outputs are mainly from the Nanjing Statistical Yearbook (NJNBS, 2013). Fire counts and intensity observed from MODIS (Moderate Resolution Imaging Spectroradiometer, https://earthdata.nasa.gov/data/near-real-time-data/firms) are used to determine the spatial and temporal distribution of emissions from biomass open burning. Regarding fugitive dust, information about individual construction sites in the city is obtained from NJEPB to improve the estimation of emission levels and spatial and temporal distributions. This includes location, period of operations, construction area, and amount of earthworks). The largest 221 construction sites in Nanjing in 2012 (accounting for 45% of the total construction area) are shown in Figure S1 (c) in the supplement. The annual activity levels for the main area sources for 2010-2012 are summarized in Table S1.

2.2 Emission factors

As mentioned previously, parameters related to emission factors for key sources (CPP, CEM, ISP, and RCP) are obtained through onsite surveys for each plant. The parameters for CPP include boiler type, combustion technology, fuel quality (sulfur,

ash, and volatile matter contents), types and pollutant removal efficiencies of APCDs (flue gas desulphurization (FGD), selective catalytic reduction (SCR)/selective non-catalytic reduction (SNCR), dust collection). Emission factors can then be determined or calculated based on the method described by Zhao et al. (2010). For cement production, the kiln type, PM removal efficiency of dust collectors, and fuel quality are investigated and emission factors are calculated following Lei et al. (2011) and Zhao et al. (2012a; 2013). For ISP, key parameters in four main processes (coking, sintering, pig iron production, and steelmaking) are obtained, including the SO_2 removal rate of FGD for sintering, PM removal rate of dust collectors, and the gas release ratios of coke ovens, blast furnaces, and basic oxygen furnaces. Emission factors for each process are then calculated following Zhao et al. (2012a; 2013). For the chemical industry, the surveyed parameters include the types and amounts of raw materials and products, the types and volumes of tanks, and technologies applied for VOC control. In particular, the emission factors for refineries are determined by industrial process, including production, storage, loading, and unloading (Wei et al., 2008; USEPA, 2002; EEA, 2013). Inter-annual variations in these parameters for major sources are tracked in the survey so that changing emission factors over time (2010-2012) can be determined. Table 1 summarizes the penetrations and removal efficiencies of APCDs for CPP and typical industries in Nanjing from 2010 to 2012. For other industrial sources, emission factors are taken mainly from the database by Zhao et al. (2011; 2013), after incorporating the most recent results from domestic measurements. Table S4 in the supplement summarizes the emission factors for main industrial processes.

For other sources for which local emission factors are currently unavailable, emission factors are determined based on existing studies in other parts of China. If no domestic studies are available, recommendations of USEPA (2002) are applied. Road dust emissions are estimated following USEPA (2002), based mainly on the average weight of vehicles, silt loading of the road surface, and traffic flow. Those parameters

are taken from Fan et al. (2007) and Huang et al. (2006), with some adjustments of road types for Nanjing. Emission factors of construction dust recommended by USEPA (2002) are used in this work, i.e., 0.026, 0.106, and 0.191 (kg/m^2)/month for $PM_{2.5}$, PM_{10}, and TSP, respectively. The mass fractions of BC and OC in construction $PM_{2.5}$ are assumed to be 2.4% and 3.4%, respectively, from measurements by Zhao et al. (2009).

For gasoline stations, Nanjing completed installation of vapor recovery systems at all stations at the end of 2012. VOC emission factors for gas storage, loading, unloading and sales are determined at 0.03, 0.87, 0.10 and 2.44 g/kg, respectively (Wei et al., 2008; Fu et al., 2013). Solvents include paints for buildings and furniture, ink, fabric coating adhesives, and pesticides. VOC emission factors for decorative adhesives, interior wall paints, and wood paints are taken from Fu et al. (2013), while those for other solvent use come mainly from Wei et al. (2008).

Emission factors for non-road transportation are mainly from Zhang et al. (2010) and Ye et al. (2014). Emission factors for household biofuel use are estimated based on results of various domestic measurements as summarized in Zhao et al. (2013) and Cui et al. (2015), while those for biomass open burning are from Li et al. (2007). NH_3 emissions from livestock farming and fertilizer use are taken from Dong et al. (2010), Yang (2008), and Yin et al. (2010).

3 RESULTS

3.1 Inter-annual variability and sector distribution of emissions

The annual emissions of various air pollutants and CO_2 from anthropogenic sources in Nanjing are shown in Figure 1(a) for 2010-2012. In 2010, the total emissions of SO_2, NO_X, CO, VOCs, NH_3, $PM_{2.5}$, PM_{10}, TSP, CO_2, BC and OC are estimated at 165, 216, 774, 224, 21, 71, 94, 158, 79976, 6.2, and 6.7 Gigagrams (Gg), respectively. Note the numbers here for PM emissions do not include fugitive dust

from construction and transportation, to facilitate comparison with inventories that omit the source. Despite large growth in coal consumption from 2010 to 2012, the emissions of SO_2 and NO_X in 2012 are estimated to be smaller than those in 2010, implying the effectiveness of emission control measures for the city in recent years. These measures include mainly the increased use of flue gas desulfurization (FGD) and selective catalytic reduction (SCR) systems in the power generation sector (see the detailed information in Table 1). The slight increase in SO_2 emissions between 2011 and 2012 resulted mainly from the growth in coal consumption in industries other than power generation, where FGD systems have not been widely deployed. For NO_X, the large increase in coal consumption from 31 million metric tons (Mt) in 2010 to 35 in 2011 dominated the growth of NO_X emissions, even with improved use of SCR in power sector. From 2011 to 2012, the growth in coal consumption was limited while the average removal efficiencies of SCR are significantly improved (as shown in Table 1), leading to reduced NO_X emissions for the whole city. PM emissions are estimated to be quite stable for the three years, with small increases in $PM_{2.5}$ and PM_{10}. Rising mass fractions of $PM_{2.5}$ to TSP (from 45% to 48%) indicate the difficulty in controlling emissions of finer primary particles compared to coarser ones. For VOCs and NH_3, which have not been well regulated in national action plans for air pollution prevention and control (Zhao et al., 2014), the inter-annual variabilities of emissions are small and driven mainly by relative stability in chemical and agricultural production, respectively. While CO_2 continues to rise, no growth is estimated for CO from 2011 to 2012, implying improved overall combustion efficiency in the city.

Figure S2 in the supplement shows the sector contributions to total emissions by year and species. From 2010 to 2012, power plants, iron & steel plants, and other industrial plants are the largest SO_2 sources, contributing 41%-42%, 14%-19%, and 32%-23% of total emissions, respectively. NO_X emissions come mainly from power plants (45%) and on-road transportation (20%) throughout the time period. The shares of SO_2 and NO_X emissions from the power sector are clearly smaller than its shares of

coal consumption (57%-64%) or CO_2 emissions (48%-57%), due largely to relatively stringent emission controls in the sector. It can be found that the sector distribution of NO_X emissions did not change much annually, even with clear enhancement of NO_X control in coal-fired power plants as shown in Table 1. The growth in coal consumption of power plants partly offset the benefits of improved penetration and removal efficiency of SCR on NO_X control, and the NO_X emissions from power sector did not vary much for the three years (97, 112 and 94 Gg for 2010, 2011, and 2012, respectively). Besides power sector, in addition, emission controls were also improved for other sources, including the increased use of retrofitted low-NO_X burner for industrial boilers, and the implementation of strict emission standards for vehicles. For example, the emissions from other industrial combustion (OIN) were estimated to decrease from 22 to 14 Gg from 2010 to 2012, and the emissions from on-road vehicles did not change a lot despite of vehicle population growth, leading to relatively small variation in sector distribution of emissions for the three years.

Fugitive dust, particularly that of road origin, is identified as the dominant anthropogenic source of PM emissions. The fugitive dust shares of TSP are estimated to range 64%-70% during the research period, while smaller fractions are found for finer particles and carbonaceous aerosols. Apart from fugitive dust, iron & steel production plays a significant role in PM emissions in Nanjing, with its shares of TSP, PM_{10}, and $PM_{2.5}$ calculated at 15%-16%, 20%-23%, and 35%-41%, respectively. This results mainly from the large coal use by the sector, and relatively poor PM control measures of certain plants compared to other major coal-consuming sources, e.g., power plants. Iron & steel production is also identified as the biggest contributor of CO emissions for the city with its share reaching 60% in 2012, even though emission factors for the sector in Nanjing (based on field investigations) are smaller than the national average (Zhao et al., 2012a). This is partly attributed to relatively little inefficient coal combustion at other sources in the city (e.g., in small industry and residential use), resulting in much lower fractions of CO emissions from those sources

than the national averages. VOCs come mainly from chemical production (52%) and solvent use (29%-30%). With vapor recovery systems increasingly applied, VOC emissions from gas stations decline during the research period. Despite an increase in vehicle population, the fractions of on-road transportation emissions for most species decrease from 2010 to 2012, attributed mainly to implementation of increasingly strict vehicle emission standards. From effective prohibition of burning of agricultural wastes, the emission contributions of this source, mainly of particles, carbonaceous aerosols, and CO, are also considerably reduced.

3.2 Spatial and temporal distribution

For simulation of atmospheric transport and chemistry, the emission inventories are allocated into a 3×3 km grid system. For sources lacking specific location information, their emissions are assumed to be correlated with population density, with the exception of NH_3, which is allocated based on the density of agricultural GDP. Shown in Figure 2 are the spatial distributions of SO_2, NO_X, $PM_{2.5}$ (exluding fugitive dust from construction and roads) and VOC emissions for Nanjing in 2012, and the locations of the ten largest point sources of each species. Relatively high emission densities are found in the urban area, particularly around certain large power generation and industrial sources. As illustrated Figure 3, the fractions of emissions from point sources for all concerned species are estimated to exceed 50%, as are those from the collective four key source types, with the exception of BC, at 38%.

Monthly distributions of SO_2 emissions by sector and that of total emissions of all species for 2012 are respectively shown in Figure S3 (a) and (b) in the supplement. Note again that fugitive dust from construction sites and roads is excluded. The results of MEIC are also provided in Figure S3(a) for comparison. It can be seen that the temporal distributions of the two studies are similar except for residential emissions, which are smaller overall in this work compared to MEIC. As indicated by MODIS fire counts, over 90% of biomass open burning occurred in May-July, leading to much

higher OC emissions in those three months compared to any other time of the year. For other species, the temporal distributions of emissions correlate closely with those of activity levels, with a drop in February attributed mainly to reduced energy supply and industrial production during the Spring Festival. Pronounced diurnal variations of on-road transportation emissions are illustrated in Figure S4 in the supplement, with two peaks at the rush hours. The daily shares of CO and VOC emissions in the morning rush hour (16%) are slightly higher than those of NO_X (14%) and $PM_{2.5}$ (15%). Based on the assumptions of COPERT, the cold start of most vehicles occurs in the morning, leading to larger CO and VOC emission factors during this time compared to those during stable operation of vehicles. The influence of vehicle cold starts on emissions of NO_X and $PM_{2.5}$ is smaller.

3.3 Comparisons with other studies in emission estimates

Figure 1(b) compares our estimates of Nanjing emissions with those from other inventories (Fu et al., 2013; MEIC) for a common year, 2010. In the other studies, national or regional average levels for some parameters related to emissions, e.g., the penetrations and pollutant removal rates of emission control devices, are applied. These values can vary considerably from those based on plant-by-plant field investigations, leading to clear differences in emission estimates compared to the current work.

Our estimate of SO_2 emissions for Nanjing is 25% and 22% higher than those of Fu et al. (2013) and MEIC, respectively, even though the plant-by-plant survey indicates an FGD penetration rate of 92% of installed power generating capacity, higher than the provincial average of 85% used in Fu et al. (2013). The higher estimate results because: 1) the total coal consumption from the Environmental Statistics applied in this work is 14% larger than that provided by the Nanjing Almanac used in other studies (NJCLCC, 2011; see Section 4.6 for more discussion); and 2) a relatively lower removal efficiency of FGD is obtained from the onsite

381 survey for 2010. Similar NO_X emission levels are found between current work and
382 MEIC, while lower emissions were provided by Fu et al. (2013). According to filed
383 survey, the penetration rate of SCR/SNCR increased from 44% to 67%, and the NO_X
384 removal efficiency increased from 18% to 77% during 2010-2012 (Table 1). The
385 penetration rate is much larger compared to the provincial average of 22% applied in
386 MEIC and Fu et al. (2013), partly offsetting a discrepancy in estimated emissions
387 caused by larger activity levels used in current city-scale inventory.

388 Our estimates for $PM_{2.5}$, PM_{10}, and BC emissions (without fugitive dust
389 emissions) are larger than those of Fu et al. (2013) or MEIC in 2010. This results
390 mainly from larger emissions from industry (particularly iron & steel production), as
391 the survey revealed that relatively old and inefficient wet dust collectors were still
392 used at some plants. OC emissions, however, are estimated to be lower than MEIC
393 indicates, due mainly to very little coal or biomass burning in the city-level statistics.

394 VOC emissions estimated in this work in 2010 are 34% larger than Fu et al.
395 (2013) and 36% larger than MEIC. In particular, emissions from refineries and
396 chemical plants, calculated using detailed information on each plant's inputs of raw
397 materials and the product types and amounts, are 116% higher than those in regional
398 inventories (Fu et al., 2013). Thus the fraction of total VOC emissions attributed to
399 industrial processes is estimated at 48% by us, larger than the YRD average level of
400 34% (Fu et al., 2013). Given Nanjing is a city with large petroleum refining and
401 chemical industries, and that much higher production of crude oil, gasoline, diesel and
402 liquefied petroleum gas is reported than in other YRD cities in 2010 (NJNBS, 2013),
403 the higher VOCs emissions indicated by the plant-based inventory is believed to
404 better reflect the city's true industrial structure.

405 For CO, our estimates are 12% higher for industry than those of MEIC, but 26%
406 and 37% lower respectively for residential and transportation sectors, resulting in 2%
407 lower emissions for anthropogenic sources as a whole. The discrepancy in sector
408 contributions is caused mainly by the high percentage of centralized coal combustion

409 in the city: power, iron & steel, cement, and chemical plants consumed over 95% of
410 the city's coal, based on our field survey. Our CO_2 emission estimate is 22% higher
411 than that of MEIC, resulting mainly from the difference in coal consumption reported
412 by the Environmental Statistics database and the city almanac.
413

414 ## 4 ASSESSMENT OF THE CITY-SCALE EMISSION INVENTORY

415 The current inventory is assessed to gauge improvements of emission estimates
416 using a city-scale framework. The inter-annual variability, spatial distributions, and
417 correlations of a number of species of the inventory are evaluated by comparison to
418 available satellite and ground observations, and to downscaled national emission
419 inventories.

420 ### 4.1 Evaluation of inter-annual trends and spatial distribution of NO_X emissions
421 with satellite observations

422 The inter-annual trend in NO_X emissions estimated bottom-up is compared with
423 that of NO_2 vertical column densities (VCDs) based on satellite observations. The
424 VCDs of tropospheric NO_2 are retrieved from the Ozone Monitoring Instrument (OMI)
425 by the Royal Netherlands Meteorological Institute (Boersma et al., 2007; 2011), using
426 monthly data with spatial resolution of $0.125^o \times 0.125^o$ (data source:
427 http://www.temis.nl/airpollution/no2col/no2regioomimonth_v2.php). Illustrated in
428 Figure 4 are annual emissions estimated in this work for Nanjing from 2010 to 2012
429 and VCDs from 2005 to 2012 for 4 regions: Nanjing, Shanghai, 4 provinces in the
430 YRD (including Jiangsu, Zhejiang, Anhui and Shanghai), and a rectangular region
431 containing Nanjing (see Figure S1(a) for reference). The first two represent NO_2 at
432 city levels while the latter two represent regional levels. To eliminate seasonal
433 variations, NO_2 VCDs are presented as 12-month moving averages, calculated as the
434 means of the data for the previous and subsequent six months. All the data are

435 normalized to the 2010 level of Nanjing. While NO_2 VCDs started declining around
436 2008 for Shanghai, it kept increasing for the rest of the YRD region including Nanjing
437 until 2012. Clearly higher than the regional levels, the average NO_2 VCD for Nanjing
438 approached that of Shanghai after 2010. This implies, on one hand, the benefits of
439 Shanghai's strict emission controls of on-road vehicles and big power plants (K.
440 Huang et al., 2014), implemented in advance of other regions. On the other hand, the
441 growth of NO_2 for the rest of the YRD demonstrates the spread of air pollution source
442 regions from major metropolitan areas to less developed cities nearby, and suggests
443 the need for increased efforts in emission and pollution abatement in those areas, as
444 indicated by Zhang et al. (2012a). Decreased emissions in Nanjing are clearly
445 indicated by this work after 2011, attributed mainly to the national policy of
446 compulsory installation and running of SCR devices in the power sector. This
447 inter-annual variation shows good consistency with that of OMI NO_2 VCD.

448 It should be noted that uncertainties exist in the comparison between the
449 inter-annual variations in emissions and VCDs and the results should be interpreted
450 cautiously. First, the biases of NO_2 VCD retrieval from OMI were reported to reach
451 40% attributed probably to the errors in the air mass factor calculations (Boersma et
452 al., 2007; 2011). Such uncertainties are potentially larger than the inter-annual
453 changes in NO_X emissions of Nanjing between 2010 and 2012, and thus weaken the
454 comparison. However, since the bottom-up emissions are not evaluated by the
455 absolute values but the relative trends of VCDs, the effects of NO_2 VCD retrieval
456 uncertainties on the comparison could partly be mitigated. Another uncertainty comes
457 from meteorology. As shown in Figure S5 in the supplement, the inter-annual changes
458 in meteorological parameters were small except for precipitation during 2010-2012 in
459 Nanjing. The varied precipitation could change the data sampling of retrieval, and
460 thereby influence the NO_2 VCD levels. Finally, the period for emission and VCD
461 comparison is relatively short. Even the NO_2 VCDs kept decreasing slightly after
462 2012, the benefits of NO_X emission control could not be fully confirmed as the

emission inventory for the most recent years are still unavailable due to the delay of activity data report. Analysis on long-term trend in emissions from the bottom-up method is further suggested for better understanding the NO_X pollution in the area.

To further assess possible improvement of emission estimates by the current city-level inventory, the spatial distribution of monthly means of OMI NO_2 VCD in summer (June-August) 2010 over Nanjing is compared with that of two emission studies: 1) city-level emissions at spatial resolution of 3×3 km by the current work, and 2) MEIC emissions developed at the provincial level with a resolution of 5×5 km. For the purpose of visualization and further analysis, the emissions are reallocated to a 0.125°×0.125° grid system from the original spatial distributions, consistent with the resolution of retrieved OMI NO_2 VCD. We assume that the NO_2 VCD from satellite observations reflect the anthropogenic NO_X emissions of the city for the following reasons. NO_X emissions in East China are predominantly anthropogenic (Mijling et al., 2013); lightning and soil sources as a share of total emissions are estimated to peak in July, when they account for 9% and 12%, respectively (Lin, 2012). NO_X emissions in Nanjing are clearly larger than in surrounding areas (Huang et al., 2011), and the NO_2 VCD over the city is believed to be most influenced by local emissions.

As shown in Figure 5, a similar spatial pattern of NO_X is captured by the gridded emissions and satellite observations, and relatively higher pollution in the urban area in the center of the city is indicated, attributed mainly to the combined effects of intensive transportation and large point sources. The emission inventories, however, underestimate the high-pollution areas compared to OMI observations, particularly MEIC. To further gauge improvement in spatial distribution by the city-scale emissions, correlations between the gridded emissions and the VCD are analyzed. As shown in Figure 6 (a), the correlation coefficients (R) between the emissions and the VCDs are calculated at 0.450 and 0.408 for this work and MEIC, respectively, indicating better agreement by the city-scale inventory. Moreover, a sensitivity test on the correlation coefficients is conducted through step-wise exclusion of the grid cells

with the largest emissions. Along with the increase in excluded grid cells, the R for this city-scale emission inventory remains above 0.43, while those of MEIC sharply decrease (Figure 6 (b)). In order to estimate emissions of the whole country, the MEIC is based mainly on energy and economic statistics at the provincial level, though it includes a limited number of major point sources, e.g., power plants with relatively good documentation and large emissions. Emissions from other point sources are based on coarser inputs due to constraints of time, labor, and data availability. The current study, in contrast, compiled detailed information for all power plants and most other industrial sources in Nanjing through comprehensive survey investigation, as described in Section 2. Better estimates of emission levels and spatial distributions should thus be expected, particularly for small or medium-size emission sources. Once the grid cells dominated by major power plants are excluded from the two inventories, as shown in Figure 6 (c), the current city-scale emissions still correlate well with satellite observations (R=0.436) while MEIC shows little correlation (R=0.085). The results reflect that inventories compiled at the provincial or regional level better estimate emissions of large sources than small or medium-sized ones, due to relative availability of information on power plants but much poorer nationwide data availability for other industrial plants. When focusing on smaller regions like cities, however, detailed information on more emission sources from onsite survey becomes crucial for improving emission estimates.

It should be noted that high NO_2 VCDs are found over the Yangtze River by OMI (roughly following the dark red zone in Figure S6 in the supplement) while current emission inventories cannot capture this. Possible underestimation of emissions from ships is indicated. Due to data limits, only ships arriving or leaving the port of Nanjing are taken into account in the current city-scale inventory, while those passing through Nanjing are omitted. Further investigation of the vessel flow along the Yangtze River is thus necessary to improve the estimation of ship emissions, which may be particularly influential at small spatial scales. Besides the ships, the

519 emissions from factories along the river could also contribute to the high VCDs.

520 **4.2 Spatial correlations between pollutant emissions and ambient concentrations**
521 **from ground observations**

522 Ambient concentrations for selected pollutants from ground observations are
523 used to test the city-scale emission inventory. Daily averages of SO_2, NO_2, CO, and
524 $PM_{2.5}$ concentrations for 2012 are obtained from the 9 state-operated monitoring
525 stations in urban/suburban Nanjing, mapped in Figure S1 (d). The SO_2, NO_2, CO, and
526 $PM_{2.5}$ concentrations were measured by Ecotech EC9850B, Ecotech EC9841B,
527 Ecotech EC9830B and Met One 1020 analyzers, respectively. The emissions of
528 specific pollutants around each site with a grid cell size of $0.04^o \times 0.04^o$ are calculated
529 from the 3×3 km gridded inventories, and correlations with annual mean
530 concentrations of corresponding species are analyzed. Since none of the city's key
531 sources (CPP, CEM, ISP or RCP) are located in those grid cells, the effects of
532 individual big sources on the correlation between emissions and observation are
533 assumed to be limited.

534 As shown in Figure 7(a), modest agreement is found in spatial patterns between
535 the observed concentrations and the emissions for SO_2 and NO_X (NO_2), with the R
536 calculated at 0.58 and 0.46, respectively. SO_2 and NO_X have average atmospheric
537 lifetimes of several days and one day, respectively, thus the ambient concentrations
538 are expected to partly reflect emission intensities nearby and the correlation analysis
539 adds support for the reliability of the city-scale emission inventory. The y-intercepts in
540 Figure 7(a) can be considered as the approximations of regional background levels of
541 SO_2 and NO_2, and the value for NO_2 is relatively high compared to SO_2. Since the
542 YRD is a developed region with large economy, high energy consumption, and,
543 particularly large vehicle population and intensive transportation, the background
544 levels of NO_2 could be enhanced, and the local emissions in Nanjing city thus have a
545 less significant impact on NO_2 concentrations. Moreover, in urban areas with plenty

of emission sources and relatively large emission density, NO was found to account for large fraction of NO_X in the ambient atmosphere (Zhou et al., 2008). As the dominating component of primary NO_X directly from emission sources, NO is more difficult to be oxidized to NO_2 in urban than in rural or remote regions, attributed to less resident time for chemistry conversion in urban. Given the 9 state-operated monitoring sites are all located in urban/suburban Nanjing, the observed NO_2 concentrations were less sensitive or correlated to the NO_X emissions, compared to the case of SO_2, and it leads to the smaller slope of ambient NO_2 levels to NOx emissions and the lower correlation coefficient in Figure 7(a).

As shown in Figure 7(b), the correlation coefficient for CO is calculated at 0.61, and it reaches 0.86 when the observation of the Caochangmen site is excluded, where extremely high emissions are calculated but low ambient levels were observed (to be further discussed in Section 4.4). Even with a longer lifetime (weeks to months) than SO_2 or NO_X, CO in the atmosphere over Nanjing results mainly from primary emissions from incomplete combustion, implying reasonable agreement between emissions and concentrations. However, emissions from small coal combustion sources still cannot be fully tracked or precisely quantified, and this evidence is thus tentative.

4.3 Evaluation of emissions against top-down constraints from observations

For certain pairs of pollutants that come from common sources and thus share emission characteristics, or weakly reactive species that are relatively stable in the atmosphere, correlations of ambient concentrations can provide useful “top-down” constraints on “bottom-up” estimates of primary emissions. In this work, the correlations of three pairs of species in the atmosphere—BC and CO, OC and EC, and CO_2 and CO—are analyzed based on daily mean concentrations from ground observations in 2012. Combining the mass or molar ratios of emissions for corresponding species allows further evaluation of the city-scale inventory.

BC and CO

BC and CO both result from incomplete combustion of solid fuels and certain industrial processes such as coking. With relatively long atmospheric lifetime, CO is usually recognized as a tracer of pollution transport. Combined with BC levels, it can also be used to test emission inventories of the two species (most at regional or national scale), which is particularly useful for BC given its relatively large emission uncertainties (Kondo et al., 2011; Wang et al., 2011; Zhao et al., 2011; 2012a). We follow the method presented in Wang et al. (2011) but focus on evaluating the city-level, top-down emission ratio of BC to CO based on observations at Caochangmen in Nanjing (point A in Figure S1(d) in the supplement). We choose this site for emission evaluation for two main reasons. First, it is an urban site and thus assumed to be more representative for the city emissions, compared to suburban/rural sites that are more influenced by emissions from broader areas. Second, Caochangmen is the biggest and the most comprehensive state-operated station in the city. Among all the 9 state-operated sites in Nanjing, it is one and only station that conducts observation not only for the six criterion pollutants (i.e., SO_2, NO_2, CO, O_3, PM_{10}, and $PM_{2.5}$) but also for certain species including BC used here and CO_2 used later. Daily means of BC and CO concentrations are calculated based on the hourly data from continuous observations using Magee AE 31 and Ecotech EC9830B analyzers, respectively, and the correlation between the two species are then evaluated and used to check the bottom-up emission inventories. Since ambient levels of BC and CO depend not only on emissions but also on atmospheric processes (e.g., wet and dry depositions of BC, chemical reactions of CO with OH, and mixing of both BC and CO) that exert different influences on the two species (Wang et al., 2011), the top-down emission ratio of BC to CO ($BC/CO|_{E,top\text{-}down}$) is calculated from the observed BC/CO ($dBC/dCO|_t$) by excluding the influence of the above-mentioned atmospheric processes, as indicated in Equation (2):

$$dBC/dCO|_t = BC/CO|_{\text{E,top-down}}\, F_{\text{dry}}\, F_{\text{chem}}\, F_{\text{mixing}}\, F_{\text{wet}} \quad (2)$$

F_{wet} indicates the wet deposition screening. Based on precipitation data from the Weather Underground weather site (http://www.wunderground.com/history/), the data in precipitation days were excluded to eliminate the effects of wet deposition. F_{dry}, F_{chem} and F_{mixing} indicate the screening of dry deposition of BC, chemical reactions of CO with OH, and mixing of both BC and CO, respectively. Following the methods by Wang et al. (2011), F_{mixing} is set at 1 and $F_{chem+dry}$ is calculated at 0.88 based on the lifetime of BC and CO in the atmosphere.

As shown in Figure 8, the annual ratio of BC to CO from observations is estimated at 0.0071 $\mu gm^{-3}\, ppbv^{-1}$ by linear regression with the reduced major axis method (Hirsch and Gilroy, 1984), and it is 0.0073 $\mu gm^{-3}\, ppbv^{-1}$ if the days of wet deposition are excluded. Once influence from other atmospheric processes are further eliminated, $BC/CO|_{\text{E,top-down}}$ rises to 0.0084, lower than the ratio from the city-scale bottom-up emission inventory at 0.0097, or that from the MEIC national inventory at 0.0095. It should be noted that the downtown observation site is influenced heavily by local transportation, particularly gasoline vehicles that have relatively high CO but low BC emissions. Therefore, the top-down ratio of BC to CO observed at the site is expected to be somewhat lower than that of emissions over the entire city. The comparison of top-down and bottom-up results is thus roughly consistent with the city-scale emission inventory, although possible overestimation of BC, or underestimation of CO emissions are indicated.

Aside from mean annual levels, comparisons are also conducted for seasonal BC to CO ratios, as summarized in Table 2. The highest $BC/CO|_{\text{E,top-down}}$ is found in summer while the lowest is in winter. Such seasonal variation, however, is not indicated in the current bottom-up emission inventory, for the following possible reasons. First, as described in Section 2, the temporal distribution of emissions is based on investigation of large and medium enterprises. However, the species of concern here, especially BC, come largely from small industrial and residential

sources, for which temporal information is still lacking. For transportation, the increased cold start of vehicles in winter also leads to higher CO emissions that cannot be fully captured by COPERT (Cai and Xie, 2010; Xiao et al., 2004) and could then lead to an overestimate of BC/CO from the bottom-up method. Second, although Caochangmen is located in urban Nanjing, it would inevitably be influenced by emissions from wider regions outside the city that are not quantified in the city-scale inventory. For example, biomass burning, which has a higher BC to CO ratio than exists in the ambient atmosphere, occurs more frequently in less-developed areas such as northern Jiangsu and Anhui provinces than in Nanjing. According to MODIS, 79% of agricultural fire points in Jiangsu 2012 were found in summer, elevating the ambient BC/CO in this season. Third, uncertainty exists about the estimation of F_{chem}. In winter, the lowest OH densities in the boundary layer resulting from the weakest radiation lead to the smallest CO sink, and the opposite is true in summer (Seiler et al., 1984; Huang et al., 2013). The elevated F_{chem} in summer should thus lead to reduced $BC/CO|_{\mathrm{E,top\text{-}down}}$. In this work, however, the seasonal difference in F_{chem} cannot be precisely quantified precisely based on existing studies, and the same F_{chem} has to be used for all seasons, leading to possible overestimation of $BC/CO|_{\mathrm{E,top\text{-}down}}$ for summer and underestimation for winter.

OC and EC

EC and primary OC result from incomplete combustion, and the ratio of OC to EC concentrations is used to evaluate carbonaceous aerosol emissions and the formation of secondary organic aerosols (SOA) through the EC-tracer method (Castro et al., 1999). From 2011 to 2013, ambient EC and OC in downwind Nanjing were collected using quartz filters and analyzed with a DRI Model 2001 Thermal/Optical Carbon Analyzer by season (Li et al., 2015). The ratios of primary OC to EC, $(\mathrm{OC/EC})_{\mathrm{pri}}$, were then determined based on the observation. Attributed to limited

654 sampling size, Li et al. (2015) chose the lowest daily OC/EC during the sampling
655 period for each season as the seasonal $(OC/CE)_{pri}$, to exclude the effects of SOA (see
656 Figure S7 for the observed time series of ambient OC to EC ratio). The $(OC/EC)_{pri}$
657 were then estimated at 1.70, 1.27, 1.53, and 1.85 for spring, summer, autumn, and
658 winter, respectively, with an annual average of 1.59. In this work, we adopt those
659 results and assume that they serve as a top-down constraint of carbonaceous aerosol
660 emissions. From the bottom-up estimates, the emission ratios of OC to BC in our
661 city-scale emission inventory and MEIC are respectively 1.38 (for 2012) and 1.24 (for
662 2010, the most recent year for which MEIC emissions are available), both of which
663 are lower than the top-down $(OC/EC)_{pri}$ from observations. With few emission sources
664 nearby, the observation site is thought to be less influenced by local sources (e.g.,
665 on-road transportation that has a relatively low emission OC to BC ratio) than the
666 regional transport of pollutants (Li et al., 2015). Thus some sources with high OC to
667 BC ratios that are uncommon in Nanjing but more dispersed outside the city
668 contribute significantly to the observed concentrations at the site. Those sources
669 include residential fossil and biomass combustion and biomass open burning. The OC
670 to BC emission ratios of Jiangsu and Anhui provinces surrounding Nanjing are
671 estimated respectively at 1.91 and 2.13 (Zhao et al., 2013), clearly larger than the
672 local emission ratio of Nanjing. Moreover, the carbonaceous aerosol sampling
673 procedure used by Li et al. (2015) would lead to positive artifacts of OC measurement
674 and elevated OC to EC, since usage of quartz filters adsorbs some semivolatile
675 organic compounds (SVOC) in the ambient atmosphere (Cheng et al., 2009). The
676 system bias of OC quantification from this sampling approach was estimated to reach
677 50% in US (Chow et al., 2010; McDonald et al., 2015), and it was found to be 100%
678 in certain city in China (Hu et al., 2008). However, the bias can vary largely between
679 cities, and it has not been well quantified for Nanjing, making the evaluation of
680 emission inventories of carbonaceous aerosols less conclusive. Finally, uncertainty
681 also exists in the $(OC/EC)_{pri}$ determination by Li et al. (2015), as the sample size from

682 off-line measurements was small. To better evaluate the city-level OC and BC
683 emissions, therefore, more observational research with improved (e.g., long-term and
684 continuous) measurements is strongly recommended at sites where local sources
685 dominate, and the artifacts of the measurement should be sufficiently analyzed.

686 **CO_2 and CO**

687 CO_2 is a well-known greenhouse gas, with the main anthropogenic sources fossil
688 energy combustion and industrial processes. The ratios of CO_2 to CO emissions differ
689 between source types, reflecting varying combustion efficiencies. The observed ratio
690 of CO_2 to CO levels in the atmosphere can thus be used as an indicator of energy
691 efficiency, as well as a top-down test of emissions estimated bottom-up. The annual
692 molar ratios of CO_2 to CO emissions in Nanjing are calculated at 65.7, 73.6, and 76.1
693 for 2010, 2011, and 2012, respectively, significantly higher than that in Beijing in
694 2008 (32.8, Zhao et al., 2012a). They are also higher than the mixing ratios observed
695 in rural Beijing in 2008 (26.8, Y. Wang et al., 2010) or at Hatetuma Island (HAT), a
696 remote site located off the coast of continental East Asia and influenced by air masses
697 transported from East Asian countries from late fall to early spring (34.5, Tohjima et
698 al., 2014). Given the large discrepancy, data from measurements in urban Nanjing
699 (Caochangmen, Point A in Figure S1 (d)) are further analyzed to test the emissions.
700 Daily mean concentrations of CO_2 and CO are derived from hourly observations using
701 Thermo 410i and Ecotech EC9830B analyzers, respectively, for all of 2012. To
702 exclude the effects of biogenic emissions that prevail in warm seasons, data for the
703 winter months (January, February, and December) are used. The prevailing wind
704 directions over Nanjing in winter are east and northeast, and large point sources,
705 accounting for 64% of the city's CO_2 emissions, are located to the east and northeast
706 of Caochengmen, supporting use of the observational data for the current purpose.
707 The average observed concentrations of CO_2 and CO in winter were 421 ppmv

708 and 608 ppbv, respectively. Based on the cumulative probability distribution of daily
709 CO concentrations (as shown in Figure S8 in the supplement), the whole dataset is
710 divided into three subsets: (1) below the 30th percentile (with average CO and CO_2
711 concentrations at 350 ppbv and 410 ppmv, respectively), (2) between the 30th and 95th
712 percentile (677 ppbv for CO and 424 ppmv for CO_2), and (3) above the 95th percentile
713 (above 1200 ppbv for CO and 448ppmv for CO_2). We consider that subset (1)
714 represents air masses from relatively clean areas outside Nanjing, and subset (2) a
715 well-mixed blend of sources of CO_2 and CO over Nanjing. Subset (3) is assumed to
716 indicate extremely serious regional pollution episodes, in which pollutants were
717 trapped in a shallow inversion layer (Y. Wang et al., 2010). Subset (2) is believed to
718 best reflect the typical effects of local emissions and is used for bottom-up emission
719 comparisons.

720 Illustrated in Figure 9 is the CO_2-CO correlation estimated with the reduced
721 major axis method based on surface observations and the CO_2 to CO ratios from
722 bottom-up emission inventories for Nanjing. Our estimate of the CO_2 to CO ratio
723 (76.1) is closer to observations (86.9) than MEIC (52.8), implying improvement in the
724 current city-scale inventory. The observed CO_2 to CO ratio, however, should
725 theoretically be lower than that from emissions for the following three reasons. First,
726 compared to CO, the observation of CO_2 at an urban site would be more influenced by
727 sources within a broader region than the city, as CO_2 has a longer lifetime in the
728 atmosphere. Thus it is not fully representative of the very centralized and large CO_2
729 emissions inside the city, particularly those from large point sources (e.g., 17 power
730 plants and 2 iron & steel plants, which are estimated to account for 78% of total CO_2
731 emissions in Nanjing), and the CO_2 to CO ratio from observations should be reduced.
732 Second, the current emission inventory includes only the primary CO emissions while
733 there may be a fair amount of secondary CO from the oxidation of NMVOC. Duncan
734 et al. (2007) estimated that CO from NMVOC oxidation equaled nearly 50% of global
735 primary CO emissions. Given the intensive refineries and chemical plants and thereby

736 elevated NMVOC emissions in Nanjing, considerable secondary CO from NMVOC
737 oxidation can be expected, leading to a lower ratio of CO_2 to CO from observations
738 than that from primary emissions. To partly exclude the effects of NMVOC oxidation,
739 we recalculated the ambient CO_2 to CO ratio at 91.9 based on the hourly
740 concentration data from 6pm to 6am for subset (2), when the temperature was lower
741 and photochemistry was slower. The value is larger than 86.9 based on daily average
742 concentration data, attributed mainly to less formation of secondary CO. Third, as
743 discussed previously, the Caochangmen site is influenced heavily by local
744 transportation that exhibits a lower CO_2 to CO emission ratio than industry. We
745 believe that the higher CO_2 to CO ratio from observations than bottom-up emissions
746 reflect the uncertainties from both approaches. On one hand, emissions from certain
747 species and sectors need to be further improved, e.g., CO from vehicles might be
748 underestimated by the current work, since relatively poor management of vehicle
749 emissions in China cannot be tracked by COPERT. On the other hand, we speculate
750 that possible bias also exists in observations, with more discussion to follow in
751 Section 4.4.

752 The larger molar ratios of CO_2 to CO in Nanjing than in Beijing, both from
753 observations and emissions, are attributed mainly to the structure of emission sources.
754 Nanjing is a city with intensive heavy industry, and over 90% of coal was consumed
755 by power plants, iron & steel plants, cement plants, and large chemical enterprises
756 with relatively high energy efficiencies, leading to elevated ratios of CO_2 to CO in
757 emissions and thereby concentrations. Transportation, particularly gasoline vehicles,
758 is additionally a significant emission source of CO compared to CO_2, and plays
759 important roles in molar ratios of CO_2 to CO. For instance, Y. Wang et al. (2010)
760 found significantly increased ambient CO_2/CO in September 2008 (46.4 ppmv/ppmv)
761 compared to September 2005-2007 (23–29 ppmv/ppmv) in Beijing, resulting mainly
762 from the temporary ban of vehicles for the Beijing Olympic Games and thereby
763 decreased CO emissions. In 2012 the vehicle population in Beijing was 3.5 times that

of Nanjing (NJNBS, 2013). Transportation was estimated to contribute 29%-37% of anthropogenic CO emissions in Beijing from various studies (MEIC; Zhao et al., 2013), but the value is much smaller in Nanjing (10%), elevating the molar ratio of CO_2 to CO in the city.

4.4 Evaluation of local ground observations based on the city-scale emission inventory

While ground observations can be used as top-down constraints on emissions, we suggest that a high-resolution emission inventory can also be used to evaluate observational data. Although detailed local information demonstrably improves emission estimation, inconsistencies still exist between the city-scale emission inventory and ground observations of CO at Caochangmen. These inconsistencies include: 1) the significant increase in correlation coefficients between CO emissions and ambient concentrations at state-operated monitoring sites when the data at Caochangmen are excluded (from 0.61 to 0.86), as described in Section 4.2 and Figure 7(b); and 2) the higher CO_2/CO from observations at Caochangmen than that from city-scale emissions, which contradicts expectations based on atmospheric chemistry principles, as described in Section 4.3 and shown in Figure 9. This suggests the possibility of instrumental or other error reflected in the relatively low CO concentrations observed at Caochengmen in 2012. Thus we conduct a comparison of CO concentrations between Caochangmen and another state-operated site, Shanxilu, for 2012 and 2014. Similar to Caochangmen, Shanxilu is also an urban site, 3.5 km from Caochangmen. Frequency histograms of hourly CO concentrations at the two sites for 2012 and 2014 are shown in Figure S9. It can be seen that CO levels at Caochangmen were significantly lower than those at Shanxilu in 2012 (Figure S9(a)) but the CO levels were quite similar at the two sites in 2014 (Figure S9(b)). Moreover, a clear difference (~30%) in CO levels between 2012 and 2014 were found at Caochangmen (Figure S9(c)) but not at Shanxilu (Figure S9(d)). Given the very close

791 distance and similar characteristics of the two sites, we tentatively assume that there
792 should not be a significant difference in CO levels between them. Thus we conduct a
793 sensitivity test by increasing the CO concentrations at Caochangmen by 30% in 2012,
794 and repeat the assessment of the city-scale emission inventory with the revised CO
795 dataset. The correlation coefficient between CO emissions and ambient concentrations
796 at the 9 state-operated sites would be increased substantially, from 0.62 to 0.83. The
797 ratio of CO_2 to CO in winter from the revised observational data would decrease from
798 to 86.9 to 66.8, close to and lower than the ratio from the bottom-up city-scale
799 inventory (76.1), consistent with the expectation that observed CO_2/CO should be
800 smaller than emissions. If only hourly data from 6pm to 6am are applied to mitigate
801 the effects of secondary CO formation from NMVOC oxidation, an even closer
802 ambient CO_2 to CO ratio to emission inventory result would be estimated at 70.7.
803 Such data revision is clearly speculative, but encourages further analysis when
804 observational data for a longer period become available at both sites. The city-scale
805 emission inventory may thus provide a basis to raise questions about the quality of
806 local ground observations, which should not be taken for granted.

807 **4.5 Comparison between city and national inventories for certain sources**

808 To further explore the effects of methods and data employed in emission
809 estimation at city and national levels, we conduct comparisons of emission levels and
810 spatial distributions between the current inventory and MEIC for given pollutants
811 from typical sources, including SO_2 from power generation, NO_X from transportation,
812 and $PM_{2.5}$ from industry, for 2010 in Nanjing. Our estimates are reallocated to a
813 resolution of 5×5 km, the same as MEIC, so that spatial correlations between the two
814 inventories can be quantified.

815 As shown in Figure 10(a), relatively good correlation in the spatial distributions
816 of SO_2 emissions from power generation is found for the two inventories, with the R
817 estimated at 0.74. The result indicates consistency between the emission estimates of

818 the two studies for large point sources, as might be expected given their shared
819 reliance on relatively transparent, publicly available information on power plants
820 nationwide. Lacking detailed field investigation of individual sources, however,
821 national inventory studies have to rely on standard information for which routine
822 updates or revisions are not guaranteed, and the latest changes in individual plants,
823 including the closure of small power units or relocation of some power plants, cannot
824 be tracked fully or on a timely basis. This is reflected by a number of data points in
825 Figure 10(a) with positive emission values on one axis but zero on the other.
826 Regarding the total emission levels, MEIC is 35% lower than our estimate, attributed
827 mainly to the different SO_2 removal efficiencies of FGD applied in the two studies.
828 Based on the field measurement data that were reported by individual plants and
829 verified by the local environmental protection bureau, the average removal efficiency
830 of FGD for power plants in Nanjing in 2010 is estimated at 66%, lower than the
831 values commonly applied by researchers in national emission assessments (e.g., above
832 70%, Zhao et al., 2013). The discrepancy reveals the value of site-specific
833 investigation of key parameters influencing emission estimates, including the
834 SO_2-removal rate of FGD.

835 For NO_X from transportation, the spatial R is calculated at 0.652 between the two
836 estimates, and the value would rise to 0.75 if the two grid cells with the largest
837 emissions in the city-scale inventory were excluded, as shown in Figure 10(b). Similar
838 to the power sector, the general spatial pattern of emissions from transportation for the
839 two inventories is largely consistent. The emissions in MEIC, however, are much
840 more concentrated in downtown urban regions compared to our estimate, resulting
841 from differences in spatial densities of population versus transportation flows based
842 on road networks. The former is commonly applied in spatial distribution of national
843 emission inventories while the latter, when available through field investigation or
844 real-time recording, are used in city-scale ones like ours. The total NO_X emissions
845 from transportation estimated by MEIC are 27% lower than those by the city-scale

inventory, suggesting introduction of considerable uncertainty when emissions estimated at the national level are downscaled to the city level based on proxies like population or economic activity.

In contrast to the above two cases, little correlation is found between the two estimates in the spatial distribution of $PM_{2.5}$ emissions from industrial sources (Figure 10(c)). Shown in the maps of Figure 10(c) are not only the $PM_{2.5}$ emissions but also the locations of the 20 largest emitting industrial enterprises. A clear discrepancy is observed between the distribution of those sources and emissions from MEIC, while much stronger consistency is found in the current work. Without sufficient information on individual sources, inventories developed at the national level tend to allocate large fractions of emissions into urban regions with relatively high densities of population and/or economic activity, assuming good spatial correlation between emissions and those proxies. Such correlation, however, likely weakens as pollution control in urban regions is implemented because it includes significant relocation of emission sources to suburban or rural areas (a primary element of urban pollution control policy in China). The total $PM_{2.5}$ emissions from industrial sources estimated by MEIC are 50% lower than our estimate, moreover, because: 1) a national emission inventory based on the sector-average levels of controls and emission factors cannot capture atypical, extremely large sources (super emitters); and 2) coal consumption from the official statistics used by MEIC is much lower than the aggregate of individual sources evaluated in the field survey (3.0 versus 5.0 Mt for Nanjing, 2010). Comparisons and correlation analyses between inventories developed at different spatial scales, therefore, show the advantages of thorough investigation of individual emission sources, particularly for cities with many large industrial enterprises like Nanjing.

4.6 Uncertainty assessment of city-scale emission inventory

The uncertainties of China's national emission inventories have been estimated

using Monte-Carlo simulation, as described in our previous studies (Zhao et al., 2011; 2013). Targeting city scale, however, the uncertainty of current inventory for Nanjing is more difficult to be systematically quantified, as many emission factors are city- or device-dependent and their probability distributions could not be fully defined without sufficient field measurement records. In general, the uncertainties of emissions from power and industry sectors are expected to be reduced compared to the national level, as the "key sources" in the city contribute significantly to the fuel consumption and production of those sectors. As described in Section 2, the activity levels and emission factors for those key sources were complied plant by plant or obtained through onsite survey, leading to relatively small biases in emission estimation. For most area sources, the emission factors used in this work were hardly improved compared to previous national/regional inventories, thus large uncertainties remain in those sources. Given the tiny fractions of emissions by those sources in Nanjing, however, their contribution on the uncertainty of total city emissions is expected to be limited. Very high uncertainty is expected for fugitive dusts that are generally not included in national/regional inventory, as little local information is available to improve the emission factors. Given the large shares of fugitive dusts to primary PM emissions (Figure S2), field measurements on construction sites and road dusts are suggested for better emission estimation in Nanjing.

We try further to identify some common sources of uncertainty in the development of city-level emission inventories, including: 1) the inconsistencies of activity-level data from various sources; and 2) the downscaling of activity data or emissions due to lack of city-level information.

There has been continuing concern about the accuracy and reliability of China's energy statistics for more than a decade (Sinton, 2001). Statistics from various sources report divergent energy consumption levels for the country, and the choice of activity-level data for emission inventories continues to be debated. For example, China's total energy use from national statistics has been inconsistent with that

aggregated from provincial statistics, driving considerable differences in national emission estimates (Akimoto et al., 2006; Guan et al., 2012; Zhao et al., 2013). While Akimoto et al. (2006) concluded that an emission inventory based on province-by-province statistics were in better agreement with satellite observations, Guan et al. (2012) indicated that over-reporting in provincial energy statistics could be a factor. At the city level, however, there are far fewer evaluations of the accuracy of energy statistics. We find a clear discrepancy in energy consumption data in statistical sources for Nanjing: the total coal consumption in 2010 was reported at 27.9 Mt in the Nanjing Almanac (NJCLCC, 2011), while the value from the Environmental Statistics was 14% higher, 31.9 Mt. The disparity results mainly from differences in data collection for small emission sources (enterprises). While data reporting systems and resulting data quality have been gradually improved for large- and medium-scale enterprises, many small-scale ones still do not maintain well-documented records on energy consumption, and the energy use of those enterprises is poorly captured by the city almanac (personal communications with officials from Nanjing Municipal Commission of Economy and Information Technology, 2014). Aimed at pollution control, the environmental statistical system obtains and verifies energy data for each enterprise through field surveys, and we thus believe that these energy consumption data are more complete and reliable for emission inventory development. The uncertainty from such varied statistical sources could be reduced as retirement of small boilers and/or closure of small enterprises increases. Although the Nanjing Almanac stopped reporting coal consumption for the city after 2010, the Environmental Statistics indicates that the combined share of coal consumption by large- and medium-sized sources increased from 84% in 2010 to 91% in 2012, attributed to closure of small enterprises reporting highly uncertain energy data during the period.

Besides problems in the energy data, uncertainty in the city-scale emission inventory can also result from lack of information on certain industrial sectors in the

city statistics. If field surveys of individual sources cannot be conducted due to labor or time constraints, emissions have to be estimated by downscaling national or provincial estimates. To evaluate the resulting uncertainty, air pollutant emissions from non-ferrous metal smelting and the production of brick and lime in Nanjing 2012 are recalculated by the downscaling provincial estimates method (method B). In this method, emissions in Jiangsu province are first calculated based on the provincial statistics and provincial average levels of emission control. Emissions in Nanjing are then obtained according to Nanjing's fraction of certain proxy (industrial GDP in this case) out of the whole province. The results are compared with those based on detailed source investigations (method A). Shown in Table 3 are the product output (activity level) and pollutant emissions estimated by methods A and B. The activity levels estimated from provincial-level information are much higher than the actual industrial production aggregated from individual plants, suggesting downscaling produces emission overestimates. For example, gaseous pollutant emissions calculated with method B are 2, 10, and 30 times larger than those produced by method A for brick, lime, and copper production, respectively. For PM emissions, the discrepancies in emissions between the two methods are smaller, attributed partly to the compensating effects of divergent removal efficiencies of dust collectors applied in the two methods, obtained either from plant-by-plant surveys (method A) or from national or provincial average levels (method B). The differences are believed to reflect disparities in the considerable fractions of total emissions from OIN (i.e., industrial sources excluding iron & steel, cement, and chemical plants, for which information is relatively clear, as defined in Section 2.1), specifically 6%, 22%, 15%, and 24% of SO_2, NO_X, $PM_{2.5}$, and CO for lime production, as shown in Table 3. The results suggest relatively large uncertainties in city-level emission estimates lacking sufficient individual source information. In this case, moreover, the overestimates in Nanjing's emissions from downscaling provincial emissions would inevitably lead to underestimates for other cities within the province, weakening understanding of

957 emission sources and the quantitative basis of regional control policies.

958

959 # 5 POLICY IMPLICATIONS

960 ## 5.1 The effects of pollution control policies on emission abatement and air quality

961 Substantial efforts have been undertaken in specific Chinese sectors to achieve
962 national targets in both energy conservation and emission reduction (Zhao et al.,
963 2013). Under the air pollution control measures, clear benefits in emission abatement,
964 particularly in the power and transportation sectors, are found for Nanjing from 2010
965 to 2012, a relatively short period. In the power sector, electricity generation increased
966 by 58% during 2010-2012 while that specifically from coal-fired plants grew by 47%,
967 reflecting the switch of coal to gas combustion and other diversification of power
968 generation in the city. Meanwhile, coal consumption of the power sector increased by
969 only 25%, much slower than the resulting electricity generation, reflecting improved
970 energy efficiency due to replacement of small and old power units with larger and
971 more energy-efficient ones. As shown in Figure S10(a) in the supplement, the capacity
972 share of large units (above 300 MW) increased from 72% in 2010 to 78% in 2012
973 while that of small ones (below 100 MW) decreased from 20% to 16%. The
974 penetration of large units raised as well the use of APCD for SO_2, NO_X, and PM,
975 leading to significant reduction of emission factors by 30%, 23%, and 22%,
976 respectively. The decrease in emission factors can also be seen for vehicles. With
977 implementation of staged emission standards for new vehicles from 2010 to 2012, the
978 emission factors of SO_2, NO_X, CO, and VOCs are estimated to have declined by 66%,
979 33%, 34%, and 37% for gasoline vehicles (Figure S10(b)), those of NO_X, CO, and
980 VOCs by 12%, 13%, and 24% for diesel vehicles (Figure S10(c)), and those of CO
981 and VOCs by 25% and 34% for motorcycles (Figure S10(d)), respectively. The SO_2,
982 CO, and VOCs emissions from on-road transportation decreased by 39%, 11%, and

983 27%, respectively, while the vehicle population increased by 27% in the city over the
984 three years.
985 The benefits of emission control on air quality can be partly confirmed by
986 comparisons of changes in emissions and ambient concentrations. During August
987 16-24, 2013 when the 2nd Asian Youth Games (AYG) were held in Nanjing, a series of
988 extra emission controls measures were undertaken by the government to improve air
989 quality for the Games. Those measures included increasing use of low-sulfur coal at
990 power plants, closing small factories with relatively large pollutant emissions,
991 stopping construction in some regions, and restricting traffic. Taking these extra
992 measures into account, the emissions of SO_2, NO_X, $PM_{2.5}$, PM_{10}, and CO over August
993 16-24, 2013 are estimated to have declined 23%, 31%, 21%, 14%, and 33%,
994 respectively, compared to those in the same period in 2012, based on the monthly
995 distributions described in Section 3.2 (see Table S5 in the supplement).
996 Correspondingly, the daily average concentrations for those pollutants in Nanjing
997 during the AYG period were found to decline by 22%, 27%, 10%, 5%, and 22%,
998 respectively, compared to the same period in 2012 (Yu et al., 2014). Although changes
999 in other factors including meteorological conditions also influenced air quality, the
1000 consistency between the reduced emissions and concentrations suggests that local
1001 emission abatement played a primary role in the air quality improvement.

1002 **5.2 Effects of super emitters and small sources on emission levels and spatial**
1003 **distributions**

1004 For cities with intensive, heavily polluting industries like Nanjing, large point
1005 sources with significant energy consumption and/or industrial production are
1006 estimated to dominate the levels and spatial distribution of emissions of the city. As
1007 shown in Figure 3, the areas with high emission densities in Nanjing are in good
1008 agreement with geographical locations of point sources for all pollutants. The ten
1009 largest point sources of SO_2 emissions are estimated to account for 54% of total

emissions in the city (Figure 2(a)), and the analogous number for NO_X is 43% (Figure 2(b)). For $PM_{2.5}$, as shown in Figure 2(c), the ten largest sources are estimated to be responsible for 75% of total primary emissions in Nanjing (excluding construction and road dust). In particular, extremely high emissions are found for iron & steel plants, resulting mainly from the high production of steel and reliance on wet scrubbers with relatively low removal efficiencies (annual average of 85%) in the exhaust streams of basic oxygen furnaces. Similarly, the ten largest refineries and chemical plants shown in Figure 2(d) are responsible for 52% of VOC emissions in Nanjing. The dominant roles of these big sources on emission levels and spatial distributions indicate that careful investigation and analysis of source-specific parameters relevant to emissions from these super emitters (e.g., removal efficiency of APCDs) are particularly crucial to the reliability of city-scale emission inventories.

Although large point sources dominate emissions at the city level, the contributions from scattered small sources cannot be overlooked. As shown in Figure 3, the fractions of air pollutant emissions from power, cement, iron & steel, and chemical plants to the city's total emissions are estimated to range from 38% to 88%, significantly lower than that of coal consumption (96%). Despite the tiny share of coal use, decentralized small coal combustion sources have a relatively high proportion of emissions, resulting from poorer emission control technologies and management than big enterprises. Regarding emission abatement and air quality improvement, it is imperative to expand pollution control from large sources to small- and medium-sized enterprises, as the potential for further reductions from the major sources are diminishing due to near-saturation of APCDs. As for improvement of emission inventories, more varied and uncertain emission factors for small boilers and kilns result from much greater diversities of manufacturing technologies. This necessitates more field measurements in the future to inform the application of emission factors in inventories and to better understand the emission characteristics of small sources.

6 CONCLUSION

With updated methods and substantial new data on local emission sources, a city-scale emission inventory of air pollutants and CO_2 is developed for Nanjing for three years, 2010-2012. Through plant-by-plant onsite surveys, emission factors, spatial and temporal emission distributions, and estimates of total emissions for major sources (power, cement, iron & steel, and refineries and chemical plants) are especially improved. Emissions in the city are dominated by large point sources, or super emitters. Despite large increases in energy consumption and industrial production, the emissions of most concerned pollutants were largely stable during the period, particularly SO_2 and NO_X, attributed to increased use and air pollutant removal rates of APCDs under national policies of air pollution control. The current estimates are consistent with the inter-annual variability of NO_2 VCD observed from OMI. The improvement of emission estimates by city-scale assessment is further indicated by analyses of spatial correlations with observations by satellite (for NO_X) and ground stations (for SO_2, NO_X, and CO), as well as by top-down constraints (BC/CO, OC/EC, and CO_2/CO) provided by ground-based observations. Analyses of bottom-up emission inventories, moreover, can identify possible errors in observational datasets, encouraging further investigation.

Limitations remain in the current work. First, some available and potentially valuable information cannot yet be fully exploited to improve emission estimates. CEMS data help to determine the time distribution of emissions, for example, but are currently less useful for estimating absolute emission levels, due to incompleteness and systematic errors in relevant parameters (e.g., flue gas flow rate). Second, since emission factors for some sources are still based on provincial or national assessments due to lack of local information, the uncertainties of the city-scale emission inventory have not yet been systematically quantified. In particular, the degree of uncertainty in the city-scale inventory compared to that of national ones remains unknown. Finally,

it is currently difficult to assess emissions of some species believed to have high emission uncertainty, e.g., VOC and NH_3, due to lack of sufficient instrumental observations. More field measurements of both emissions and ambient levels of these species are thus recommended in the future.

ACKNOWLEDGEMENT

This work was sponsored by the Natural Science Foundation of China (41205110), Natural Science Foundation of Jiangsu (BK20140020 and BK2012310), Jiangsu Science and Technology Support Program (SBE2014070918), Ministry of Science and Technology of China (2011BAK21B00), and Ministry of Education of China (20120091120019). We would like to thank Hongxin Bao and Danning Zhang from NJEPB for technical support of this work, and Jintai Lin from Peking University for comments on satellite observation, and TEMIS for free use of their monitoring data. Thanks also go to two anonymous reviewers for their very valuable comments to improve this work. The contents of this paper are solely the responsibility of the authors and do not necessarily represent the official views of the sponsors.

REFERENCES

Akimotoa, H., Oharaa, T., Kurokawac, J. I., and Horii, N.: Verification of energy consumption in China during 1996–2003 by using satellite observational data, Atmos. Environ., 40, 7663–7667, 2006.

Boersma, K. F., Eskes, H. J., Dirksen, R. J., van der A, R. J., Veefkind, J. P., Stammes, P., Huijnen, V., Kleipool, Q. L., Sneep, M., Claas, J., Leitao, J., Richter, A., Zhou, Y., and Brunner, D.: An improved tropospheric NO_2 column retrieval algorithm for the Ozone Monitoring Instrument, Atmos. Meas. Tech., 4, 1905-1928, 2011.

Boersma, K. F., Eskes, H. J., Veefkind, J. P., Brinksma, E. J., vander A, R. J., Sneep, M., van den Oord, G. H. J., Levelt, P. F., Stammes, P., Gleason, J. F., and Bucsela, E. J.: Near-real time retrieval of tropospheric NO_2 from OMI, Atmos. Chem. Phys., 7, 2103–2118, 2007.

Cai, H., and Xie, S. D.: Determination of emission factors from motor vehicles under different emission standards in China, Acta Scientiarum Naturalium Universitatis Pekinensis, 3, 319-326, 2010 (in Chinese).

Castro, L. M., Pio C.A., Harrison, R. M., and Smith. D. J. T.: Carbonaceous aerosol in urban and rural European atmospheres: estimation of secondary organic carbon concentrations, Atmos. Environ., 33, 2771-2781, 1999.

Cheng, Y., He, K. B., Duan, F. K., Zheng, M., Ma, Y. L., and Tan, J. H.: Measurement of semivolatile carbonaceous aerosols and its implications: A review. Environ. Int., 35, 674-681, 2009.

Chow, J. C.; Watson, J. G.; Chen, L. W. A.; Rice, J.; Frank, N. H.: Quantification of $PM_{2.5}$ organic carbon sampling artifacts in US networks. Atmos. Chem. Phys., 10, 5223-5239, 2010.

Cui, H., Mao, P., and Zhao, Y.: Patterns in atmospheric carbonaceous aerosols in China: emission estimates and observed concentrations. Atmos. Chem. Phys. Discuss., 15, 8983-9032, 2015.

Dong, W. X., Xing, J., and Wang, S. X.: Temporal and spatial distribution of anthropogenic ammonia emissions in China, Environmental Science, 31, 1457-1463, 2010 (in Chinese).

Duncan, B. N., Logan, J. A., Bey, I., Megretskaia, I. A., Yantosca, R. M., Novelli, P. C., Jones, N. B., and Rinsland, C. P. (2007), Global budget of CO, 1988–1997: Source estimates and validation with a global model, J. Geophys. Res., 112, D22301, doi: 10.1029/2007JD008459.

European Environment Agency (EEA), COPERT 4-Computer Programme to Calculate Emissions from Road Transport, User Manual (Version 9.0), 2012.

European Environment Agency (EEA). EMEP/CORINAIR Emission Inventory Guidebook-2013, available at http://www.eea.europa.eu//publications/emep-eea-guidebook-2013, 2013

Fan, S. B., Tian, G., Li, G., and Shao, X.: Emission characteristics of paved roads fugitive dust in Beijing, Environmental Science, 28, 2396-2399, 2007 (in Chinese).

Fu, X., Wang, S., Zhao, B., Xing, J., Cheng, Z., Liu, H., and Hao, J.: Emission inventory of primary pollutants and chemical speciation in 2010 for the Yangtze River Delta region, China, Atmos. Environ., 70, 39-50, 2013.

Guan, D., Liu, Z., Geng, Y., Lindner, S., and Hubacek, K.: The gigatonne gap in China's carbon, Nat. Clim. Change, 2, 672–675, 2012.

Hirsch, R. M., and E. J. Gilroy.: Methods of fitting a straight-line to data-Examples in

water resources, Water Resour. Bull., 20, 705-711, 1984.

Hua, L., Guo, J., Xu, Z. Y., Hu, Y. Q., Huang, Y., and Zou, B. D: Analysis of PM_{10} source profiles in Beijing, Environmental Monitoring in China, 22, 64-71, 2006 (in Chinese).

Huang, C., Chen, C. H., Li, L., Cheng, Z., Wang, H. L., Huang, H. Y., Streets, D. G., Wang, Y. J., Zhang, G. F., and Chen, Y. R.: Emission inventory of anthropogenic air pollutants and VOC species in the Yangtze River Delta region, China, Atmos. Chem. Phys., 11, 4105-4120, 2011.

Huang, K., Fu, J. S., Gao, Y., Dong, X, Y., Zhuang, G. S., and Lin, Y. F.: Role of sectoral and multi-pollutant emission control strategies in improving atmospheric visibility in the Yangtze River Delta, China, Environ. Pollut., 184, 426-434, 2014.

Huang, R. J., Zhang, Y., Bozzetti, C., Ho, K. F., Cao, J. J., Han, Y., Daellenbach, K. R., Slowik, J. G., Platt, S. M., Canonaco, F., Zotter, P., Wolf, R., Pieber, S. M., Bruns, E. A., Crippa, M., Ciarelli, G., Piazzalunga, A., Schwikowski, M., Abbaszade, G., Schnelle-Kreis, J., Zimmermann, R., An, Z., Szidat, S., Baltensperger, U., Haddad, I. E., and Prevot, A. S.: High secondary aerosol contribution to particulate pollution during haze events in China, Nature, 514, 218-222, 2014

Huang, X., Huang, X. X., Wang, T. J., Zhuang, B. L., Li, S., Xie, M., Han, Y., Yang, X. Q., Sun, J. N., Ding, A. J., and Fu, Z. B.: Observation and analysis of urban upper atmospheric carbon monoxide in Nanjing, China Environmental Science, 33, 1577-1584, 2013.

Huang, Y. M.: Study on the emission estimation and spatial distribution of urban fugitive dust, Master thesis, East China Normal University, Shanghai, 2006 (in Chinese).

Hu, M., Deng, Z., Wang, Y., Lin, P., Zeng, L., Kondo, Y., and Zhao, Y.: Comparison of EC/OC in $PM_{2.5}$ between filter sampling off-line analysis and in situ on-line measurement, Environmental Science, 29, 3297-3303, 2008 (in Chinese).

Kim S.-W., Heckel A., Frost G.J., Richter, A., Gleason, J., Burrows, J. P., McKeen, S., Hsie, E.-Y., Granier, C., and Trainer, M.: NO_2 columns in the western United States observed from space and simulated by a regional chemistry model and their implications for NO_x emissions, J. Geophys. Res., 114, D11301, doi: 10.1029/2008JD011343, 2009.

Kondo, Y., Oshima, N., Kajino, M., Mikami, R., Motcki, N., Takegawa, N., Verma, R. L., Kajii, Y., Kato, S., and Takami, A.: Emissions of black carbon in East Asia estimated from observations at a remote site in the East China Sea, J. Geophys. Res., 116, D16201, doi: 10.1029/2011JD015637, 2011.

Kurokawa, J., Ohara, T., Morikawa, T., Hanayama, S., Janssens-Maenhout, G., Fukui, T., Kawashima, H., and Akimoto, H.: Emissions of air pollutants and greenhouse gases over Asian regions during 2000–2008: Regional Emission inventory in Asia (REAS) version 2, Atmos. Chem. Phys., 13, 11019-11058, 2013.

Lei, Y., Zhang, Q., Nielsen, C. P., and He, K. B.: An inventory of primary air pollutants and CO_2 emissions from cement industry in China, 1990–2020, Atmos. Environ., 45, 147-154, 2011.

Li, X. H, Wang, S. X., Duan, L., Hao, J. M, Li, C., Chen, Y. S., and Yang, L.: Particulate and trace gas emissions from open burning of wheat straw and corn stover in China, Environ. Sci. Technol., 41, 6052-6058, 2007.

Li, B., Zhang, J., Zhao, Y., Yuan, S. Y., Zhao, Q. Y., Shen. G. F., and Wu, H. S.: Seasonal variation of urban carbonaceous aerosols in a typical city Nanjing in Yangtze River Delta, China, Atmos. Environ., 106, 223-231, 2015.

Lin, J.: Satellite constraint for emissions of nitrogen oxides from anthropogenic, lightning and soil sources over East China on a high-resolution grid, Atmos. Chem. Phys., 12, 2881-2898, 2012.

McDonald, B. C., Goldstein, A. H., and Harley, R. A.: Long-term trends in California mobile source emissions and ambient concentrations of black carbon and organic aerosols, Environ. Sci. Technol., 49, 5178-5188, 2015.

Mijling, B., van der A, R. J., and Zhang, Q.: Regional nitrogen oxides emission trends in East Asia observed from space, Atmos. Chem. Phys., 13, 12003-12012, 2013.

National Bureau of Statistics of China (NBSC): China Statistical Yearbook, Beijing, China Statistics Press, 2013 (in Chinese).

Nanjing Bureau of Statistics (NJNBS): Statistical Yearbook of Nanjing, Beijing, China Statistics Press, 2013 (in Chinese).

Nanjing Committee of Local Chronicles Compilation (NJCLCC): Nanjing Almanac, Nanjing, Editorial Department of Nanjing Almanac, 2011.

Ohara, T. A. H. K., Akimoto, H., Kurokawa, J. I., Horii, N., Yamaji, K., Yan, X., and Hayasaka, T.: An Asian emission inventory of anthropogenic emission sources for the period 1980–2020, Atmos. Chem. Phys., 7, 4419-4444, 2007.

Seiler, W., Giehl, H., BRUNKE, E. G., and Halliday, E.: The seasonality of CO abundance in the Southern Hemisphere, Tellus B, 36(4), 219-231, 1984.

Sinton, J. E.: Accuracy and reliability of China's energy statistics, China Econ. Rev., 12, 373–383, 2001.

Streets, D. G., Bond, T. C., Carmichael, G. R., Fernandes, S. D., Fu, Q., He, D.,

Klimont, Z., Nelson, S. M., Tsai, N. Y., Wang, M. Q., Woo, J.-H., and Yarber, K. F.: An inventory of gaseous and primary aerosol emissions in Asia in the year 2000, J. Geophys. Res., 108, 8809, 2003.

Timmermans, R. M. A., Denier van der Gon, H. A. C., Kuenen, J. J. P., Segers, A. J., Honoré, C., Perrussel, O., Builtjes, P. J. H., and Schaap, M.: Quantification of the urban air pollution increment and its dependency on the use of down-scaled and bottom-up city emission inventories, Urban Climate., 6, 44-62, 2013.

Tohjima, Y., Kubo, M., Minejima, C., Mukai, H., Tanimoto, H., Ganshin, A., Maksyutow, S., Katsumata, K., Machida, T., and Kita, K.: Temporal changes in the emissions of CH_4 and CO from China estimated from CH_4/CO_2 and CO/CO_2 correlations observed at Hateruma Island, Atmos. Chem. Phys., 14, 1663-1677, 2014.

U.S. Environmental Protection Agency (USEPA): Compilation of Air Pollutant Emission Factors (AP-42), fifth edition, available at http:// http://www.epa.gov/ttnchie1/ap42/, 2002.

Wang, L. T., Wei, Z., Yang, J., Zhang, Y., Zhang, F. F., Su, J., Meng, C. C., and Zhang, Q.: The 2013 severe haze over southern Hebei, China: model evaluation, source apportionment, and policy implications, Atmos. Chem. Phys., 14, 3151-3173, 2014.

Wang, L., Zhang, P., Tan, S., Zhao, X., Cheng, D., Wei, W., Su, J., and Pan, X.: Assessment of urban air quality in China using air pollution indices (APIs), Journal of the Air & Waste Management Association., 63, 170-178, 2013.

Wang, S., Zhao, M., Xing, J., Wu, Y., Zhou, Y., Lei, Y., He, K., Fu, L., Hao, J.: Quantifying the air pollutants emission reduction during the 2008 Olympic Games in Beijing, Environ. Sci. Technol., 44, 2490-2496, 2010.

Wang, Y. X., Wang, X., Kondo, Y., Kajino, M., Munger, J. W., and Hao, J. M.: Black carbon and its correlation with trace gases at a rural site in Beijing: Top-down constraints from ambient measurements on bottom-up emissions, J. Geophys. Res., 116, D24304, doi: 10.1029/2011JD016575, 2011.

Wang, Y. X., Munger, J. W., Xu, S., McElroy, M. B., Hao, J. M., Nielsen, C. P., and Ma, H.: CO_2 and its correlation with CO at rural site near Beijing: implications for combustion efficiency in China, Atmos. Chem. Phys., 10, 8881-8897, 2010.

Wei, W., Wang, S. X., Chatani, S., Klimont, Z., Cofala, J., and Hao, J. M.: Emission and speciation of non-methane volatile organic compounds from anthropogenic sources in China. Atmos. Environ., 42, 4976-4988, 2008.

Xiao, J, H., Ma, Wei., Wang, J, X., and Wang, X, W.: A simulation of cold start emission characteristics of gasoline engine with Euro- III cycle on engine test bench, Automotive Engineering, 6, 639-647, 2004 (in Chinese).

Yang, Z. P.: Estimation of ammonia emission from livestock in China based on mass-flow method and regional comparison, Master thesis, Peking University, Beijing, 2008 (in Chinese).

Ye, S. Q., Zheng, J. Y., Pan, Y. Y., Wang, S. S., Lu, Q., and Zhong, L. J.: Marine emission inventory and its temporal and spatial characteristics in Guangdong Province, Acta Sci. Circum., 34, 537-547, 2014 (in Chinese).

Yin, S. S., Zheng, J. Y., Zhang, L. J., and Zhong, L. J.: Anthropogenic ammonia emission inventory and characteristic in the Pearl River Delta region, Environmental Science, 31, 1146-1151, 2010 (in Chinese).

Yu, Y. Y., Xie, F. J., Lu, X. B., Zhu, Z. F., and Shu, Y.: The environmental air quality condition and the reason analysis during the Asian Youth Games of Nanjing, Environmental Monitoring and Forewarning, 6, 5-17, 2014 (in Chinese).

Zhang, L. J., Zheng, J. Y., Yin, S. S., Peng, K., and Zhong, L. J.: Development of non-road mobile source emission inventory for the Pearl River Delta region, Environmental Science, 31, 886-891, 2010 (in Chinese).

Zhang, Q., Geng, G. N., Wang, S. W., Richter, A., and He, K. B.: Satellite remote sensing of changes in NOx emissions over China during 1996–2010, Chinese. Sci. Bull., 57, 2857-2864, 2012a.

Zhang, Q., He, K., and Huo, H.: Cleaning China's air, Nature, 484, 161-162, 2012b.

Zhang, Q., Streets, D. G., Carmichael, G. R., He, K., Huo, H., Kannari, A., Klimont, Z., Park, I., Reddy, S., Fu, J. S., Chen, D., Duan, L., Lei, Y., Wang, L., and Yao, Z.: Asian emissions in 2006 for the NASA INTEX-B mission, Atmos. Chem. Phys., 9, 5131-5153, 2009.

Zhao, P. S., Feng, Y. C., Jin, J., Han, B., Bi, X. H., Zhu, T., and Zhang, X. L.: Characteristics and control indicators of fugitive dust from building construction sites, Acta Science Circumstantiae, 29(8), 1618-1623, 2009 (in Chinese).

Zhao, Y., Zhang, J., and Nielsen, C. P,: The effects of energy paths and emission controls and standards on future trends in China's emissions of primary air pollutants. Atmos. Chem. Phys., 14, 8849-8868, 2014.

Zhao, Y., Zhang, J., and Nielsen, C. P.: The effects of recent control policies on trends in emissions of anthropogenic atmospheric pollutants and CO_2 in China. Atmos. Chem. Phys., 13, 487-508, 2013.

Zhao, Y., Nielsen, C. P., McElroy, M. B., Zhang, L., and Zhang, J.: CO emissions in China: uncertainties and implications of improved energy efficiency and emission control, Atmos. Environ., 49, 103-113, 2012a.

Zhao, Y., Nielsen, C. P., and McElroy, M. B.: China's CO_2 emissions estimated from the bottom up: Recent trends, spatial distributions, and quantification of uncertainties, Atmos. Environ., 59, 214-223, 2012b.

Zhao, Y., Nielsen, C. P., Lei, Y., McElroy, M .B., and Hao, J. M.: Quantifying the uncertainties of a bottom-up emission inventory of anthropogenic atmospheric pollutants in China, Atmos. Chem. Phys., 11, 2295-2308, 2011.

Zhao, Y., Wang, S. X., Nielsen, C. P., Li, X. H., and Hao, J. M.: Establishment of a database of emission factors for atmospheric pollutants from Chinese coal-fired power plants, Atmos. Environ., 44, 1515-1523, 2010.

Zhao, Y., Wang, S.X., Duan, L., Lei, Y., Cao, P.F., and Hao, J.M.: Primary air pollutant emissions of coal-fired power plants in China: current status and future prediction. Atmos. Environ., 42, 8442-8452, 2008.

Zheng, B., Huo, H., Zhang, Q., Yao, Z. L., Wang, X. T., Yang, X. F., Liu, H., and He, K. B.: High-resolution mapping of vehicle emissions in China in 2008, Atmos. Chem. Phys., 14, 9787-9805, 2014.

Zheng, J., Zhang, L., Che, W., Zheng, Z., and Yin, S.: A highly resolved temporal and spatial air pollutant emission inventory for the Pearl River Delta region, China and its uncertainty assessment, Atmos. Environ., 43, 5112-5122, 2009.

Zhou, W., Wang X., Zhang, Y., Su, H., and Lu, K.: Current status of nitrogen oxides related pollution in China and integrated control strategy, Acta Scientiarum Naturalium Universitatis Pekinensis, 44, 323-330, 2008 (in Chinese).

FIGURE CAPTIONS

Figure 1. (a) The inter-annual variability of Nanjing emissions for 2010-2012 and (b) comparisons in annual emissions with other studies for 2010. The left-hand vertical axis indicates SO_2, NO_X, CO, VOCs, NH_3, $PM_{2.5}$, PM_{10}, TSP, and CO_2 while the right-hand indicates BC and OC. 2010(A) and 2010(B) refer to the emissions of current estimates with and without fugitive dust, respectively.

Figure 2. Spatial distribution of emissions for Nanjing 2012, with locations of largest point sources indicated. (a) SO_2; (b) NO_X; (c) $PM_{2.5}$ (fugitive dust from construction and road sources excluded) and (d) VOC.

Figure 3. The emission fractions of point sources, area sources, and on-road transportation, and those of key sources of total emissions in Nanjing, 2012

Figure 4. The inter-annual trends in NO_2 vertical column density (VCD) from OMI for selected regions (see Figure S1(a) for reference) and the bottom-up NO_X emissions for 2010-2012. All the data are normalized to 2010 level in Nanjing.

Figure 5. (a) Spatial distribution of city-scale NO_X emissions in this study, (b) summer NO_2 vertical column density (VCD) from OMI, and (c) NO_X emissions from MEIC for Nanjing, 2010. The resolution is 0.125°×0.125°.

Figure 6. Spatial correlation between NO_X emissions from city- and national-scale inventories and NO_2 vertical column density (VCD) from OMI, in Nanjing, 2010 for (a) all grids, (b) step-wise exclusion of grid cells with largest emissions and (c) grid cells without power plant emissions.

Figure 7. Linear regression of emissions and concentrations at the 9 state-operated stations in Nanjing, 2012. (a) SO_2 and NO_X/NO_2; (b) CO.

Figure 8. The correlation of daily BC and CO concentrations at Caochangmen site and the emission ratios of BC to CO from bottom-up inventories for Nanjing, 2012.

Figure 9. The correlation of daily CO_2 and CO concentrations at Caochangmen site and the emission ratios of CO_2 to CO from bottom-up inventories for Nanjing, 2012. The wintertime concentrations with CO between the 30^{th} and 90^{th} percentiles are used for the correlation analysis.

Figure 10. Spatial distribution and linear regression of emissions from city-scale and national inventories (MEIC) for (a) SO_2 from power generation, (b) NO_X from transportation, and (c) $PM_{2.5}$ from industry for Nanjing, 2010.

TABLES

Table 1. The capacity penetrations, average removal efficiencies of APCDs, and flue gas release ratios for key sources in Nanjing.

	CPP-FGD		CPP -SCR/SNCR		CEM-dust collector [a]
	Penetration	SO_2 removal efficiency	Penetration	NO_X removal efficiency	TSP removal efficiency
2010	92.4%	66.0%	43.7%	17.7%	96.9%
2011	97.0%	78.5%	66.6%	41.8%	97.0%
2012	98.3%	81.2%	67.4%	77.0%	99.6%

	ISP coke oven	ISP blast furnace	ISP sintering-FGD	ISP pig iron production-fabric filter	ISP steelmaking- dust collector [c]
	Gas release ratio [b]	Gas release ratio [b]	SO_2 removal efficiency	TSP removal efficiency	TSP removal efficiency
2010	0.5%	1.5%	70.0%	98.9%	97.3%
2011	0.5%	1.5%	70.0%	98.9%	96.7%
2012	0.5%	1.5%	70.0%	98.8%	96.7%

[a] Including the fabric filter and the electrostatic precipitator.

[b] The fraction of flue gas that is not recycled or collected for purification treatment, and is thus directly released to the atmosphere

[c] Including the fabric filter and the wet scrubber.

Table 2. The average concentrations of BC and CO and correlation of BC to CO from observations at Caochangmen and the ratios of bottom-up BC to CO emissions by season in Nanjing, 2012.

	Urban observation							Bottom-up inventory
	Avg. BC[a] (μgm^{-3})	Avg. CO[a] (ppbv)	Avg. BC[b] (μgm^{-3})	Avg. CO[b] (ppbv)	BC/CO [a] ($\mu gm^{-3}\,ppbv^{-1}$)	BC/CO [b] ($\mu gm^{-3}\,ppbv^{-1}$)	$BC/CO\|_{E,top\text{-}down}$ [c] ($\mu gm^{-3}\,ppbv^{-1}$)	$BC/CO\|_{E,bottom\text{-}up}$ ($\mu gm^{-3}\,ppbv^{-1}$)
Spring	2.946	661.3	3.009	684.9	0.0070	0.0072	0.0082	0.0101
Summer	2.644	490.3	3.000	491.0	0.0083	0.0085	0.0097	0.0096
Autumn	4.206	619.6	3.822	627.1	0.0081	0.0081	0.0092	0.0095
Winter	3.007	615.0	3.068	637.7	0.0051	0.0060	0.0068	0.0096
Overall	3.156	588.0	3.264	600.5	0.0071	0.0074	0.0084	0.0097

[a] All the observation data included.

[b] The influence of wet deposition excluded.

[c] The influence of wet and dry deposition, chemical reactions with OH radicals, and mixing excluded.

Table 3. Comparisons of emission estimations using method A (plant-by-plant survey) and B (downscaling from provincial levels) for brick, lime, and copper production in Nanjing, 2012.

	Production[1]		SO_2 emissions		NO_X emissions		$PM_{2.5}$ emissions		CO emissions	
	Method A	Method B	B/A	(B-A)/OIN[2]	B/A	(B-A)/OIN	B/A	(B-A)/OIN	B/A	(B-A)/OIN
Brick	14	29			2.0	10%	2.0	19%	2.0	13%
Lime	207	2050	9.9	6%	9.9	22%	3.6	15%	9.9	24%
Copper	1.3	39	31.1	24%			3.6	13%		

[a] The units are 10^9 bricks, 10^3 t-lime and 10^3 t-copper, respectively.

[b] Recall from Section 2.1 that OIN indicates emissions from other industry (iron & steel, cement production and chemical industry excluded) estimated at city level.

Figure 1

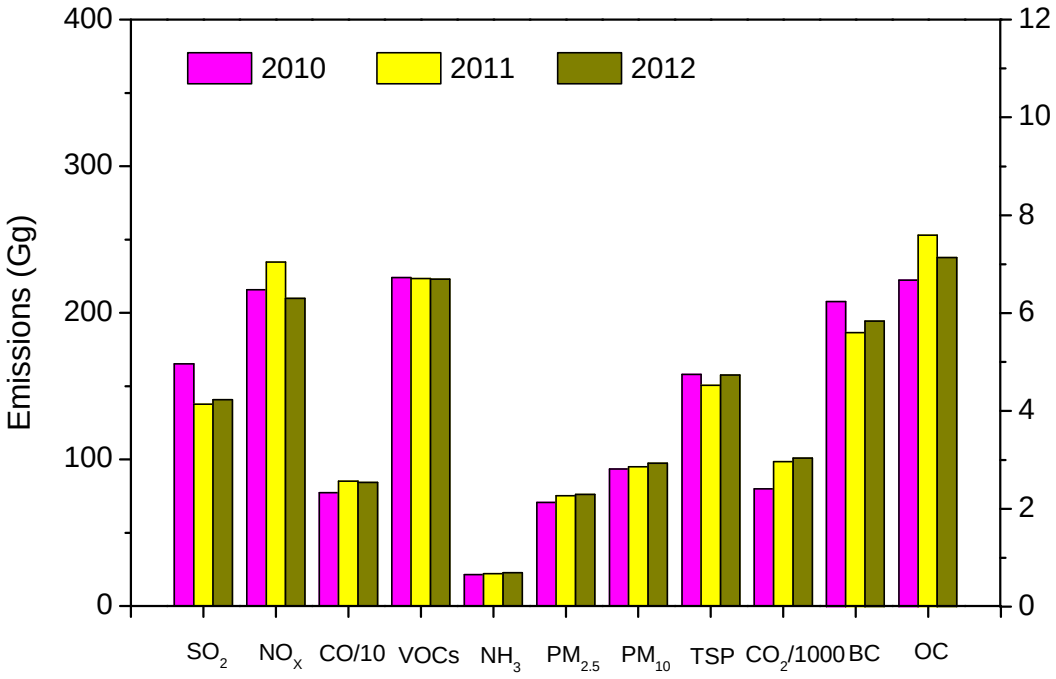
2010
2011
2012
Emissions (Gg)
400
300
200
100
0
12
10
8
6
4
2
0
SO2
NOX
CO/10
VOCs
NH3
PM2.5
PM10
TSP
CO2/1000
BC
OC

(a)

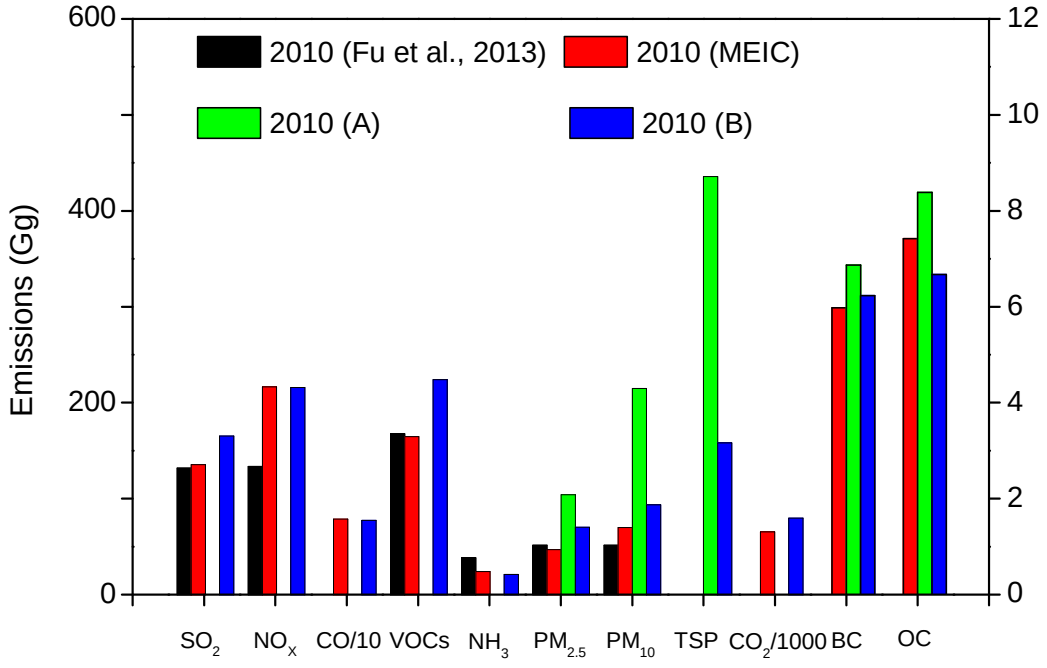
2010 (Fu et al., 2013)
2010 (MEIC)
2010 (A)
2010 (B)
Emissions (Gg)
600
400
200
0
12
10
8
6
4
2
0
SO2
NOX
CO/10
VOCs
NH3
PM2.5
PM10
TSP
CO2/1000
BC
OC

(b)

Figure 2

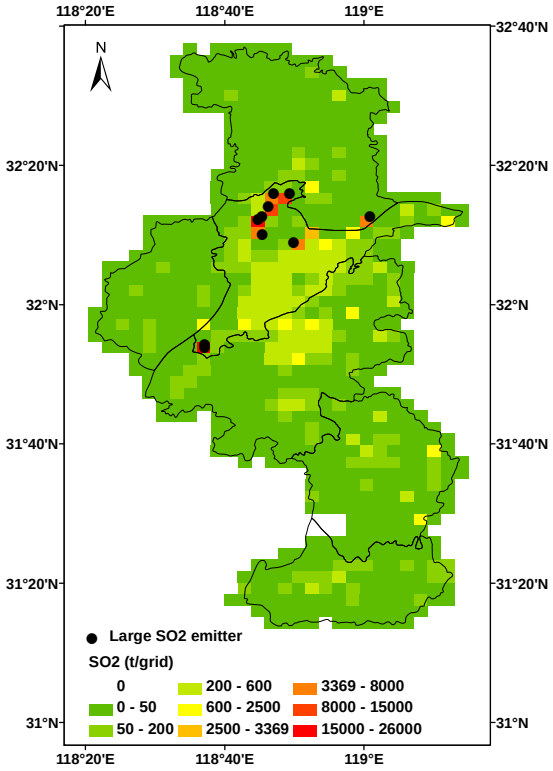

(a) SO_2

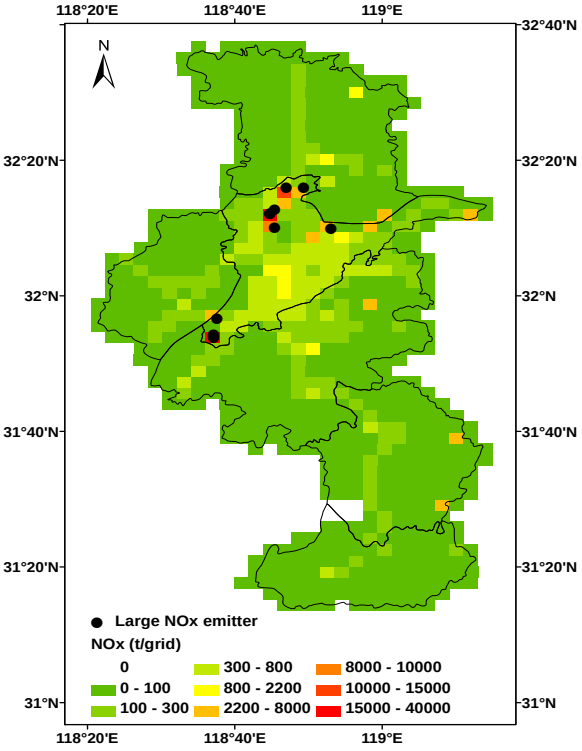

(b) NO_X

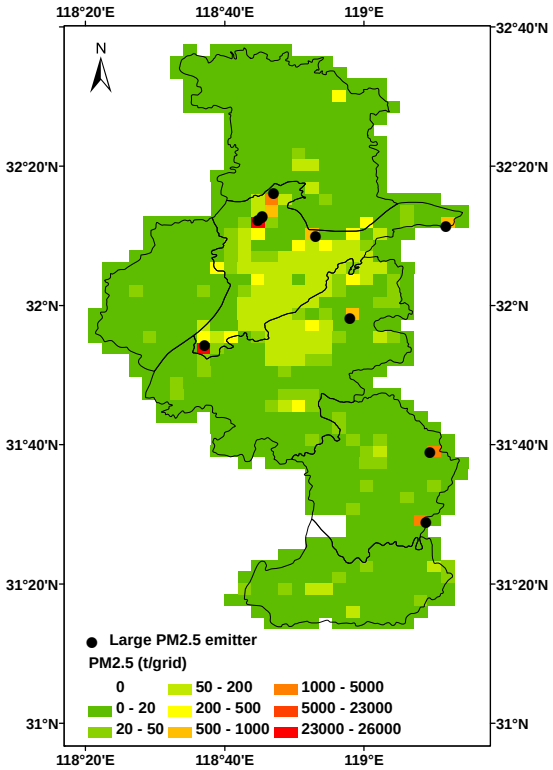

(c) $PM_{2.5}$

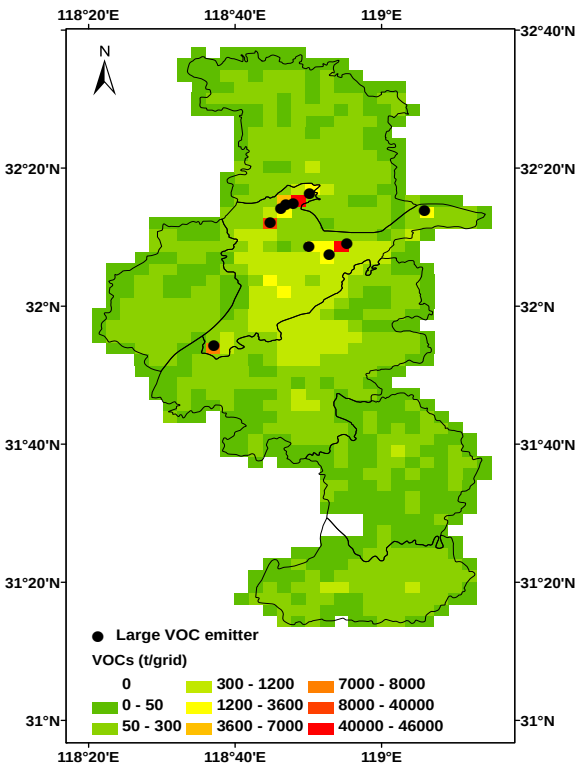

(d) VOC

Figure 3

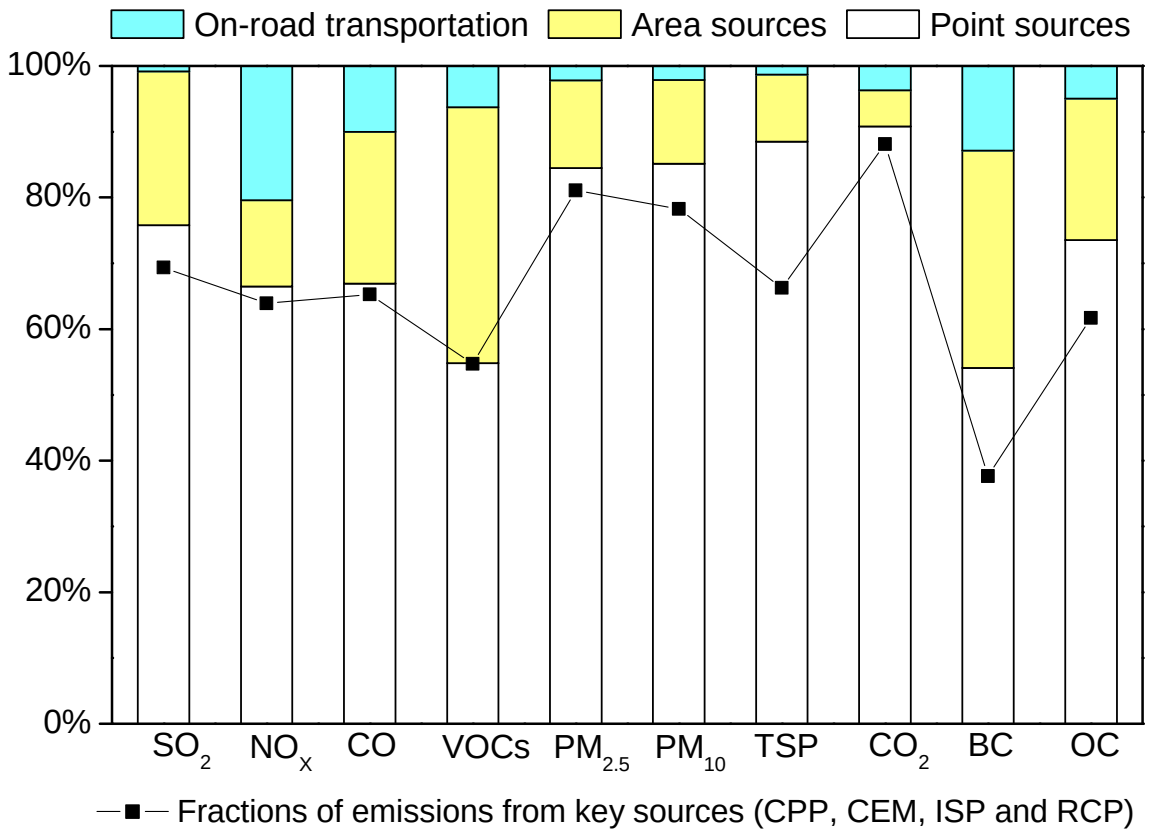
On-road transportation
Area sources
Point sources
100%
80%
60%
40%
20%
0%
SO2
NOX
CO
VOCs
PM2.5
PM10
TSP
CO2
BC
OC
Fractions of emissions from key sources (CPP, CEM, ISP and RCP)

Figure 4

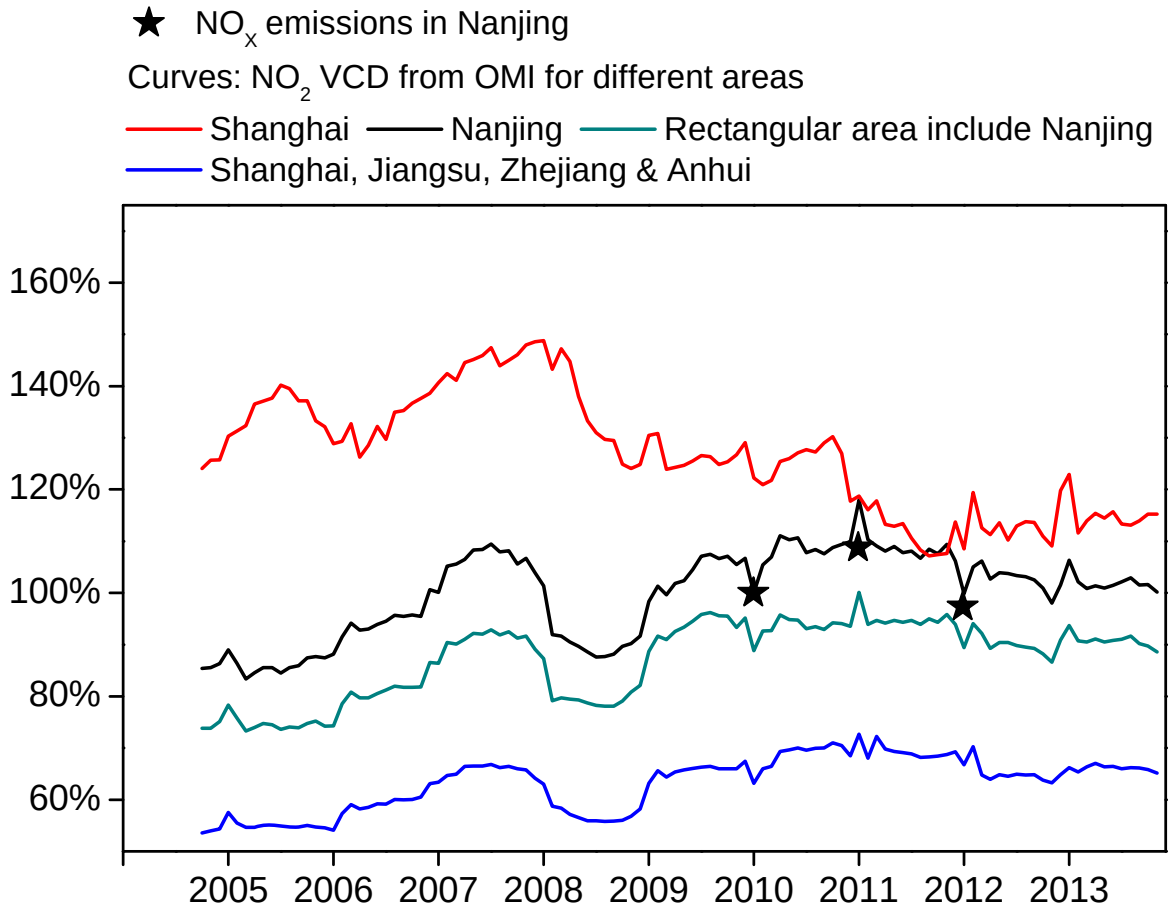
★ NO_X emissions in Nanjing
Curves: NO_2 VCD from OMI for different areas
Shanghai
Nanjing
Rectangular area include Nanjing
Shanghai, Jiangsu, Zhejiang & Anhui
160%
140%
120%
100%
80%
60%
2005
2006
2007
2008
2009
2010
2011
2012
2013

Figure 5

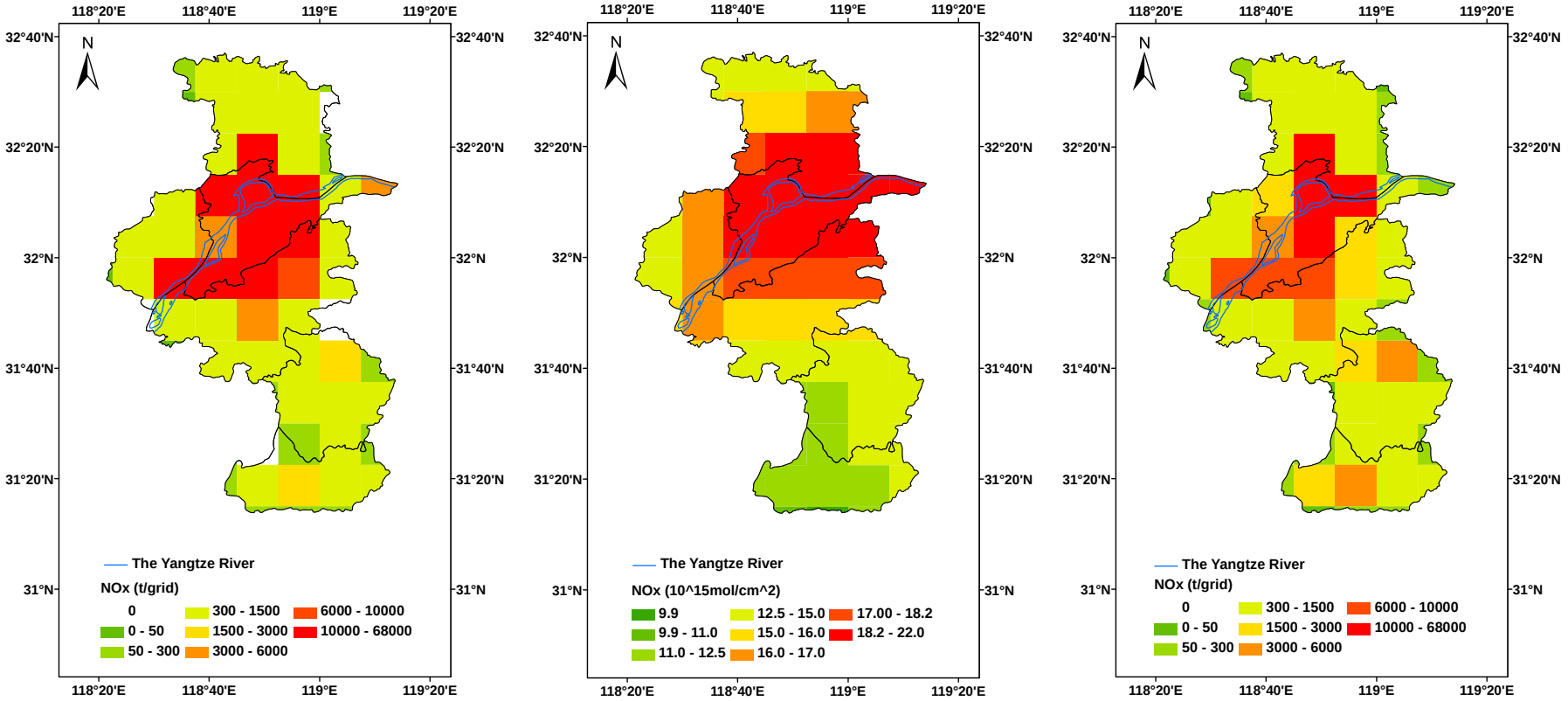

(a) Emissions: This study (b) VCD from OMI (c) Emissions: MEIC

Figure 6

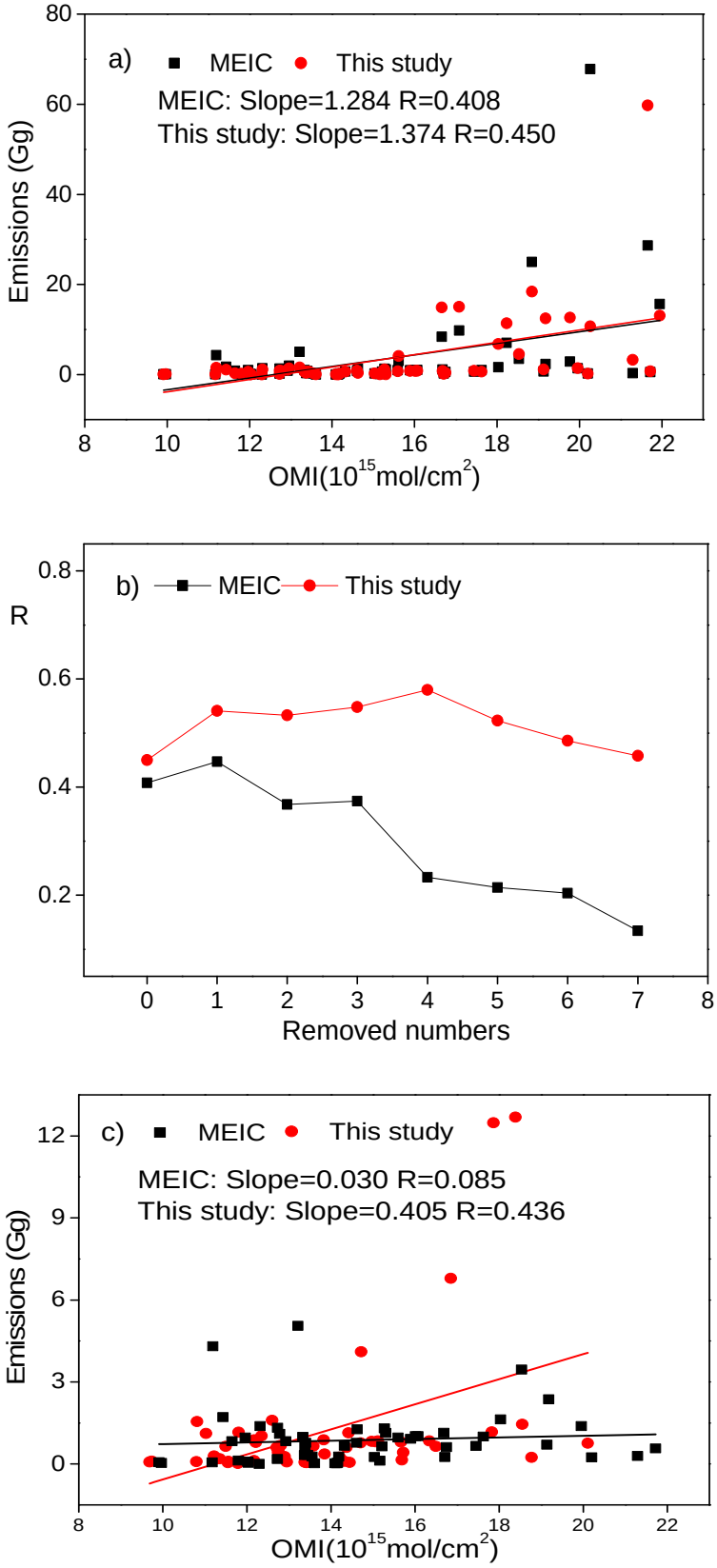
a)
MEIC
This study
MEIC: Slope=1.284 R=0.408
This study: Slope=1.374 R=0.450
Emissions (Gg)
OMI(10^15mol/cm^2)
b)
MEIC
This study
R
Removed numbers
c)
MEIC
This study
MEIC: Slope=0.030 R=0.085
This study: Slope=0.405 R=0.436
Emissions (Gg)
OMI(10^15mol/cm^2)

Figure 7

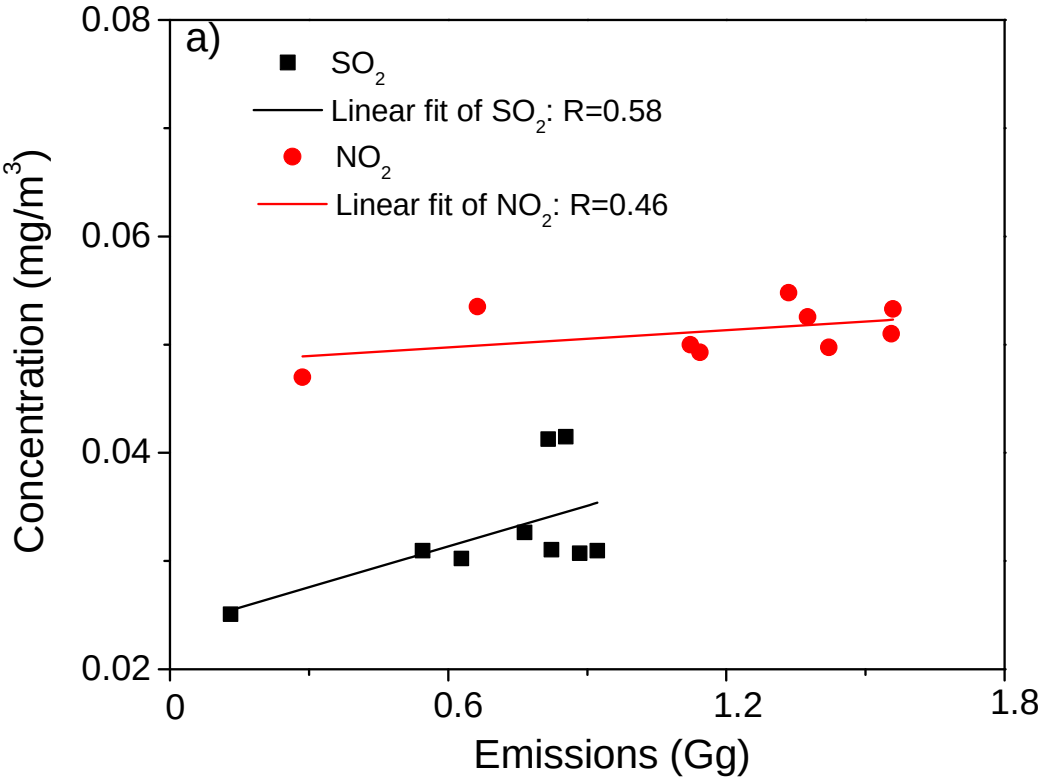
a)
SO2
Linear fit of SO2: R=0.58
NO2
Linear fit of NO2: R=0.46
Concentration (mg/m3)
Emissions (Gg)
0.08
0.06
0.04
0.02
0
0.6
1.2
1.8

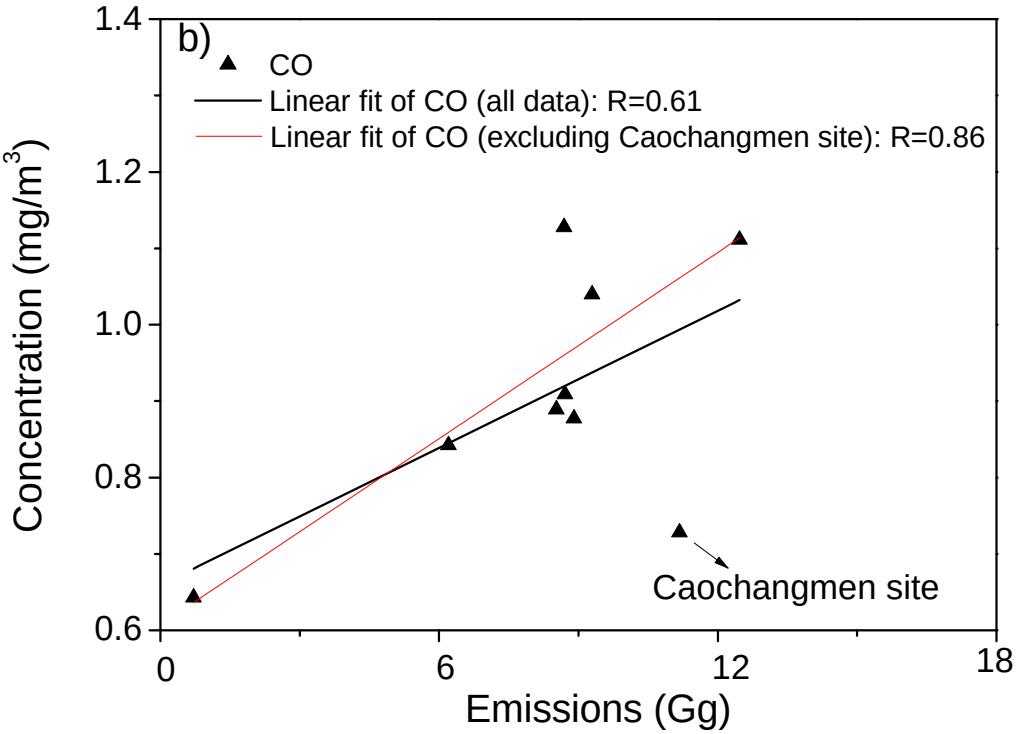
b)
CO
Linear fit of CO (all data): R=0.61
Linear fit of CO (excluding Caochangmen site): R=0.86
Caochangmen site
Concentration (mg/m3)
Emissions (Gg)
1.4
1.2
1.0
0.8
0.6
0
6
12
18

Figure 8

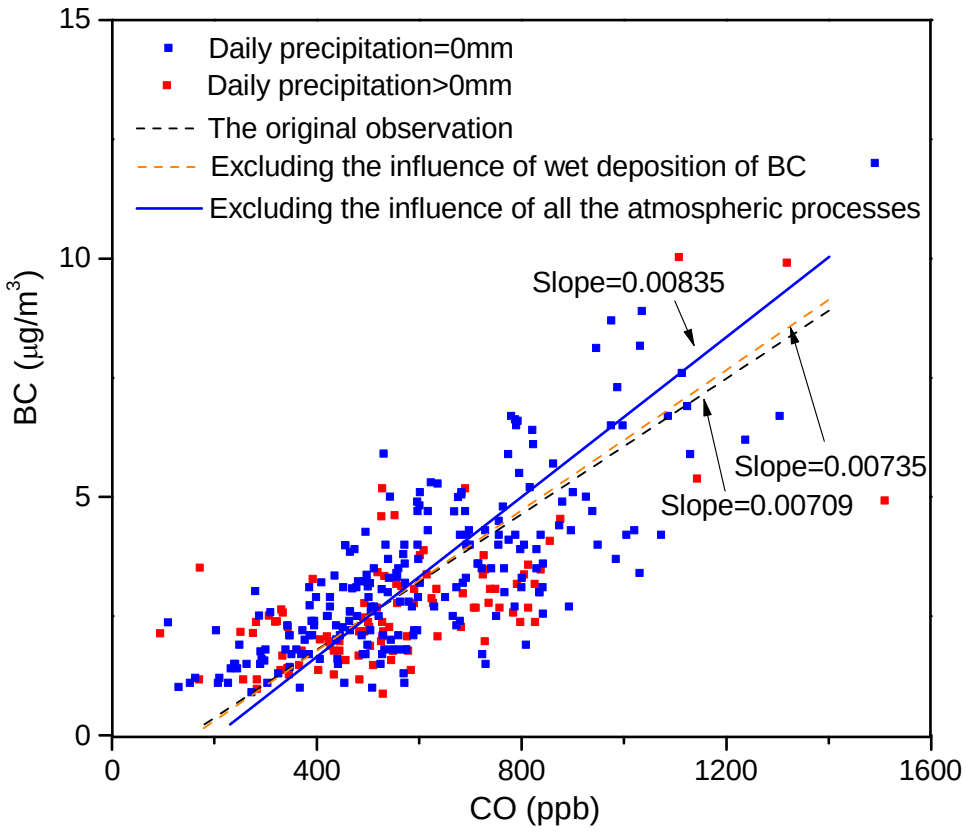
Daily precipitation=0mm
Daily precipitation>0mm
The original observation
Excluding the influence of wet deposition of BC
Excluding the influence of all the atmospheric processes
Slope=0.00835
Slope=0.00735
Slope=0.00709
BC (μg/m3)
CO (ppb)
0
5
10
15
0
400
800
1200
1600

Figure 9

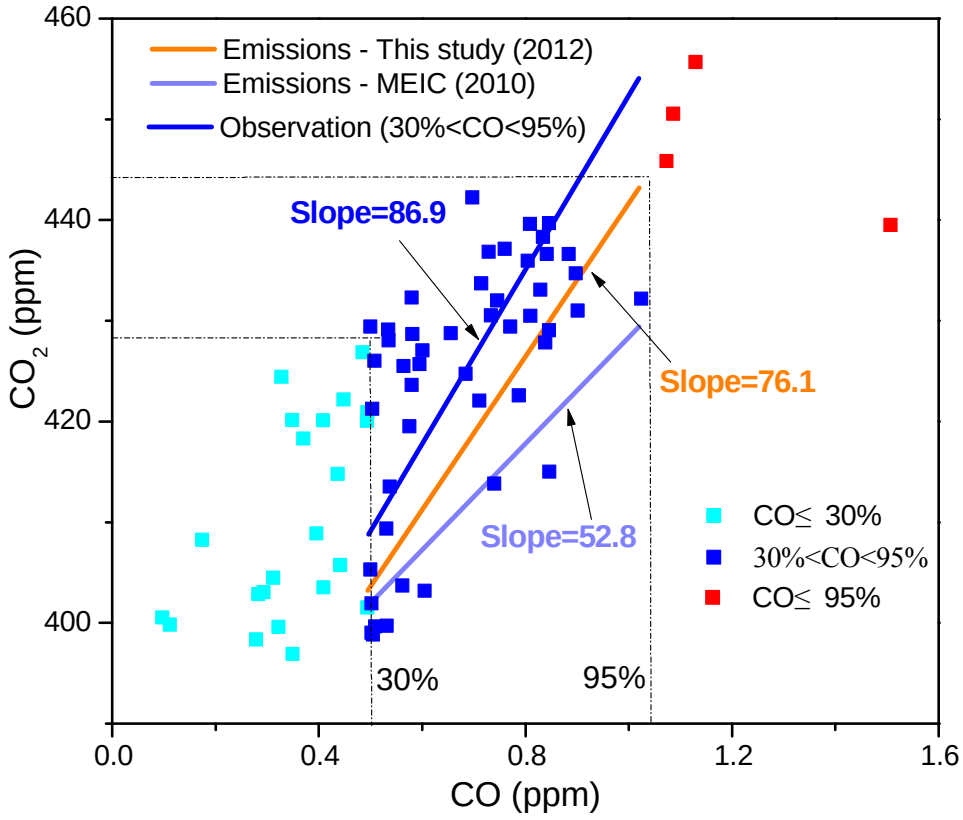
Emissions - This study (2012)
Emissions - MEIC (2010)
Observation (30%<CO<95%)
Slope=86.9
Slope=76.1
Slope=52.8
CO≤ 30%
30%<CO<95%
CO≤ 95%
30%
95%
460
440
420
400
0.0
0.4
0.8
1.2
1.6
CO (ppm)
CO2 (ppm)

Figure 10

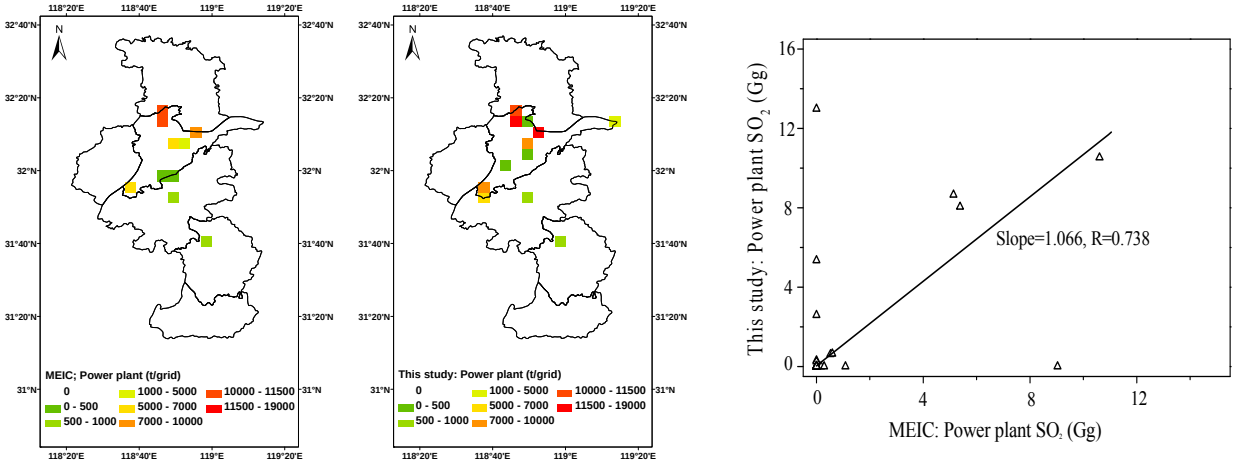

(a) Power plant: SO_2

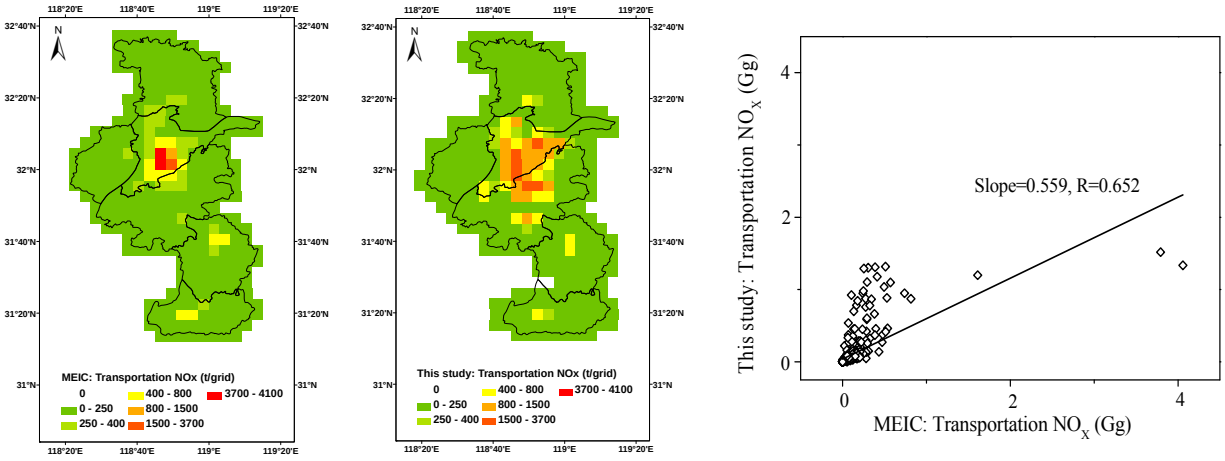

(b) Transportation: NO_X

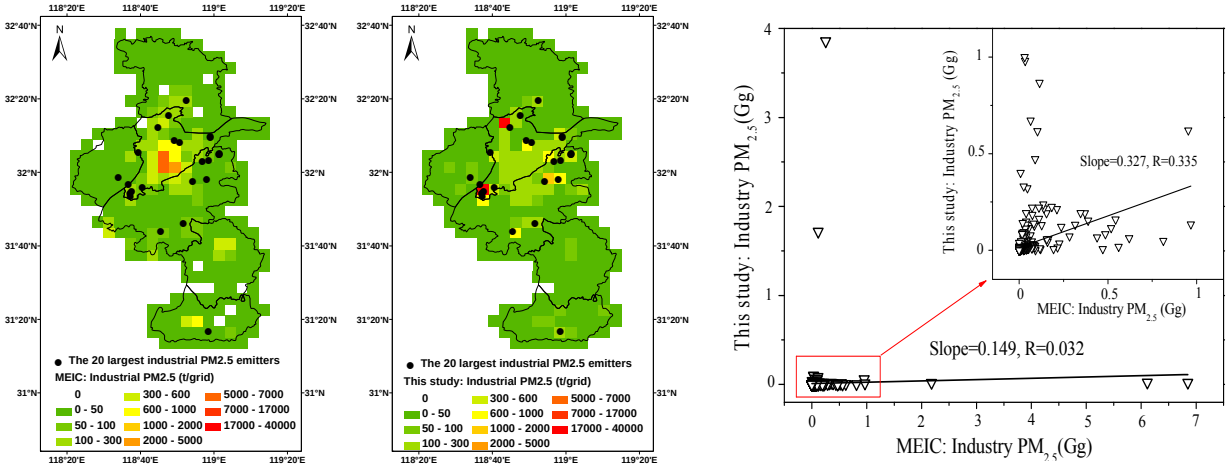

(c) Industry: $PM_{2.5}$